Observing and Modeling Precipitation in the Tibetan Plateau region

From large-scale processes to convective storms

Julia Kukulies

GÖTEBORGS UNIVERSITET

ABSTRACT

Climate change in mountain regions has far-reaching societal impacts such as increased risks for natural hazards and water scarcity that may affect billions of people in the downstream regions. Precipitation changes play a critical role in these impacts due to their effects on river runoff and flooding. However, these changes remain hard to predict due to uncertainties in climate models and a lack of reliable observations.

This dissertation aims to enhance the understanding of precipitation and its underlying large-scale and mesoscale processes in the Tibetan Plateau (TP) region, one of the most extensive and vulnerable mountain regions in the world. More specifically, the dissertation combines gauge measurements, satellite observations, reanalysis data, and high-resolution model simulations to investigate present-climate characteristics of clouds and precipitation over TP and its downstream regions.

A key outcome is a data set of large storms, so-called mesoscale convective systems (MCSs), based on two decades of high-resolution satellite observations of clouds and precipitation. This data set is used to study MCS characteristics and their relation to large-scale atmospheric circulation systems and water vapor transport. Satellite observations reveal that MCSs are important precipitation producers in the river basins surrounding the TP, while convection over the TP occurs in a more scattered manner with significantly less precipitation. In addition, satellite observations are used to evaluate kilometer-scale simulations of MCSs. The model simulations capture the general spatial pattern and magnitude of MCS-associated precipitation but show also systematic biases in MCS frequencies in some regions south and east of the TP.

It was found that interactions between large- and mesoscale processes affect the formation and evolution of MCSs over the TP and its downstream regions. The results identify several processes, e.g. interactions between the TP and the mid-latitude westerly circulation, that may drive future precipitation changes and need to be realistically represented in future climate model projections. As such, this dissertation constitutes a step towards reliable projections of climate change in the TP region.

Key words: Tibetan Plateau, Water cycle, Precipitation, Large-scale circulation, Mesoscale convective systems, Kilometer-scale climate models, Satellite observations

SAMMANFATTNING

Klimatförändringar i höga bergsområden kan leda till ökad risk för naturkatastrofer och vattenbrist och därmed orsaka stora konsekvenser för de människor som bor på och nedanför dessa bergsområden. Nederbörd är en av de komponenter i klimatsystemet som påverkar dessa risker mest. Projektioner av framtida förändringar i nederbörd i bergsområden är svåra att göra på grund av osäkerheter i klimatmodellerna och bristande meteorologiska observationer.

Syftet med denna avhandling är att öka förståelsen för nederbörden och de storskaliga och de mesoskaliga processerna som driver variationen i nederbörd på och omkring den tibetanska högplatån. Den tibetanska högplatån är en av de största och mest sårbara bergsområdena i världen och försörjer idag miljarder människor med vatten. Den föreliggande avhandlingen kombinerar information från meteorologiska stationer, satellitobservationer, återanalyser (dvs klimatdata som bygger på beräkningar utifrån historiska väderobservationer) och regionala klimatmodeller med en rumslig upplösning på kilometerskala för att studera moln- och nederbördsmönster över den tibetanska högplatån och dess omliggande avrinningsområden.

Ett viktigt resultat är en databas över mesoskaliga konvektiva stormsystem baserat på satellitobservationer från de två senaste decennier, vilken använts för att karaktärisera olika stormtyper och studera deras förhållande till den storskaliga atmosfäriska cirkulationen. Satellitdata visar att de mesoskaliga konvektiva stormsystemen står för en stor del av den totala nederbörden i de omliggande avrinningsområdena medan konvektionen på höga altituder är mer småskalig och ger upphov till förhållandevis lite nederbörd. Satellitdata användes också för att evaluera klimatmodellsimuleringarna, vilka återger det generella rumsliga mönstret och storleken på nederbörden från de mesoskaliga konvektiva stormsystemen. Simuleringarna uppvisar dock systematiska avvikelser gällande frekvensen av dessa system i vissa regioner söder och öster om den tibetanska högplatån.

Resultaten visar att interaktionen mellan processer på olika skalor påverkar bildningen och utvecklingen av stormsystemen på och runt den tibetanska högplatån. Interaktionen mellan västvindarna och bergen har exempelvis identifieras som viktiga processer vilka påverkar nutida nederbördsmönster. Eftersom förändringar i dessa processer kan orsaka framtida förändringar i nederbördsmönster, är det viktigt att de representeras på ett realistiskt sätt i klimatmodellerna. Denna avhandling är på så sätt ett steg mot bättre projektioner av klimatförändringarna på och runt den tibetanska högplatån.

LIST OF PAPERS

This dissertation is based on the following scientific papers. The papers are reprinted in their original form in the appendix and referred to in the text by their Roman numerals.

I **Kukulies** , J., Chen, D., & Wang, M. (2019). Temporal and spatial variations of convection and precipitation over the Tibetan Plateau based on recent satellite observations. Part I: Cloud climatology derived from CloudSat and CALIPSO. *International Journal of Climatology*, 39(14), 5396-5412.

II **Kukulies**, J., Chen, D., & Wang, M. (2020). Temporal and spatial variations of convection, clouds, and precipitation over the Tibetan Plateau from recent satellite observations. Part II: Precipitation climatology derived from global precipitation measurement mission. *International Journal of Climatology.*

III Lai, H. W., Chen, H. W., **Kukulies**, J., Ou, T., & Chen, D. (2020). Regionalization of seasonal precipitation over the Tibetan Plateau and associated large-scale atmospheric systems. *Journal of Climate*, 1-45.

IV **Kukulies**, J., Chen, D., & Curio, J. (2021). The Role of Mesoscale Convective Systems in Precipitation in the Tibetan Plateau region. *Journal of Geophysical Research: Atmospheres*, 126(23), e2021JD035279.

V **Kukulies**, J., Prein, A., Curio, J., Chen, D (2022). Kilometer-scale multi-physics multi-model simulations of a mesoscale convective system in the lee of the Tibetan Plateau: Implications for climate simulations *Revision submitted to Journal of Climate.*

VI **Kukulies**, J., Li, W., Chen, D (2022). Time scales of summer water vapor transport downwind of the Tibetan Plateau in reanalysis and dynamically downscaled data *Manuscript draft.*

VII **Kukulies**, J., Lai, H., Curio, J., Feng, C., Li, P., Lin, C., Sugimoto, S., Ou, T. and Chen, D. Mesoscale convective systems in the Third Pole region: characteristics, mechanisms and impact on precipitation. *Submitted to Frontiers in Earth Science.*

Author's contribution to appended articles

In **Paper I**, **II**, **IV**, **V**, **VI** Julia Kukulies designed the study, collected and analyzed the data, and wrote the manuscript. In **Paper III**, Julia Kukulies processed the satellite data, participated in the discussions about the applied methods and results, wrote sections in the method and discussion sections, helped to revise the manuscript, and approved the final version. In **Paper VII**, Julia Kukulies and Hui-Wen Lai designed the structure of the review paper, collected information, and wrote the manuscript. In addition, Julia Kukulies created the figures and coordinated the collaboration with the co-authors.

Other relevant contributions to papers

1. Zhang, X., Yin, Y., **Kukulies**, J., Li, Y., Kuang, X., He, C., and Chen, J. (2021). Revisiting Lightning Activity and Parameterization Using Geostationary Satellite Observations. *Remote Sensing*, 13(19), 3866.

2. Prein, A. F., Ban, N., Ou, T., Tang, J., Sakaguchi, K., Collier, E., Jayanarayanan, S., Sobolowski, S., Li, L., Chen, X., Zhou, X., Lai, H., Sugimoto, S., Zhou, L., Hasson, S., Ekstrom, M., Pothapakula, P., Ahrens, B., Stuart, R., Steen-Larsen, H. C., Leung, R. Belusic, D., **Kukulies**, J. , Curio, J. and Chen, D. (2022). Towards Ensemble-Based Kilometer-Scale Climate Simulations over the Third Pole Region. *Climate Dynamics*, 1-27.

3. Ou, T., Chen, D., Tang, J., Lin, C., Wang X., **Kukulies**, J. and Lai, H (2023). Wet bias of summer precipitation in the northwestern Tibetan Plateau in ERA5 is linked to weakened lower-level southerly wind over the plateau. *Climate Dynamics*, 1-15.

4. Minola, L., Zhang, G., Ou, T., **Kukulies**, J., Curio, J., Guijarro, J. A., Deng, K., Azorin-Molina, C., Shen, C., Pezzoli, A. and Chen, D (2023).Climatology of near-surface wind speed from observations and high-resolution climate models over the Tibetan Plateau. *Submitted to Climate Dynamics.*

5. Sokolowsky, G. A., Freeman, S. W., Jones W. K., **Kukulies**, J., Senf, F. Marinescu P.J., Heikenfeld, M. , Brunner, K. N., Bruning, E.C., Collis, S. M., Jackson, R. C., Leung, G. R., Pfeifer, N., Raut, B., Saleeby, S. M., Stier, P., van den Heever, S. C. (2023). tobac v1.5: Introducing Fast 3D Tracking, Splits and Mergers, and Other Enhancements for Identifying Meteorological Phenomena. *Manuscript in preparation, to be submitted to Geoscientific Model Development.*

6. Yua, H., Prein, A.F. Qic, D., **Kukulies**, J., Wang, K (2023). Kilometer-Scale Simulations Can Outperform Satellite-Based Observations in Heavy Rainfall Characteristics. *Manuscript in preparation.*

ACKNOWLEDGEMENTS

First, I would like to sincerely thank my advisor Deliang Chen for the mentorship and for giving me trust and the chance to learn about research through many exciting international projects and collaborations.

I thank my examiner Sofia Thorsson and my co-supervisor Heather Reese for their support and feedback on this thesis. I also thank Sofia and Nisse for the help with the Swedish sammanfattning.

I want to give special thanks to Andy Prein for welcoming me in Boulder and for having made my research visit at NCAR to such a great and formative experience during my Ph.D.

I full-heartedly thank all former and current colleagues at GVC, some of which have become close friends. I especially thank Michelle, Lina, and April -the inimitable GVC gals- for cozy cottage vacations and great mental support; Lorenzo for the shared office time and the infectious enthusiasm for anything; Nisse for many joyful fika hours and for always radiating calm; Salar for the worst jokes in the best moments, and, of course, for the reliable key service; my co-supervisor and scientific twin: the other Julia for the collaboration and all the chitchats in-between; Céline and Mats for nice lunches and exchanges about the academic world; Hui-Wen for helpful discussions and the nice visit together in Nanjing; and everybody else who has given me support and laughs during the past years.

Not forgotten should be all the lovely people outside of my academic bubble who I deeply thank for being a part of my life. A big thanks to my family, Lilly, Marit, Gesa, Lina, Gina, and Pooch for being there even if you are far away. Many thanks to Elin and Fanny who have accompanied me in all these years in Gothenburg. Thanks and hugs to Ingrid for many hours together in Gothenburg's forests and the beautiful piece of art that is displayed at the first page of this dissertation. And thanks to Lulu, JB, and Fra for the awesome times together, especially during the pandemic.

Finally and most importantly, I thank Simon, my partner in crime and love of my life. There are no words to describe how thankful I am for all the support, motivation, and inspiration that you have ever given me!

None of the here presented work would have been possible without the necessary tools for data processing, analysis, and visualization. Therefore, I also want to acknowledge all developers in the open-source community who make such tools available for everyone. Especially important for this dissertation were the python packages NumPy (Harris et al., 2020), xarray (Hoyer & Hamman, 2017), pandas (pandas development team, 2020), SciPy (Virtanen et al., 2020), cartopy (Met Office, 2010 - 2013), and matplotlib (Hunter, 2007). In addition, I thank the ***tobac*** *(Heikenfeld et al., 2019) developer team for the great collaboration and for inviting me to contribute and further develop a python package for cloud tracking that was used in the presented research.*

Contents

Part I

SYNTHESIS

Chapter 1

BACKGROUND AND OBJECTIVES

Mountain environments belong to the regions most affected by climate change. While melting glaciers and snow are the most evident climate change impact in mountain regions, precipitation changes play another critical role because of their effects on river runoff and natural hazards (Hock et al., 2019). Changes in water supply and flood risk resulting from changing precipitation patterns may affect several billion people that live in the downstream regions and depend on water from mountains (Immerzeel et al., 2020). Despite their societal relevance, precipitation changes over mountains are among the least understood climate change impacts. This is of because of complex interactions between mountains and precipitation processes that are poorly understood, even in the present climate. A solid understanding of the climate processes affecting precipitation changes is crucial to create reliable future projections of precipitation in mountain regions.

This dissertation aims to improve the understanding of the atmospheric processes that influence precipitation over and around the Tibetan Plateau, a region that is highly relevant for water resources in East Asia. In particular, large-scale atmospheric processes and the role of convective storms are investigated through multiple observations and high-resolution climate models.

The following introductory chapters present the dissertation topic through the lens of anthropogenic global climate change. More specifically, this chapter explains why mountain regions are a particular focus in recent climate research, how mountain regions and precipitation are affected by climate change, and what these changes imply for the Tibetan Plateau region.

1.1 Mountain environments as global hotspots of climate change

1.1.1 Climatic changes and physical drivers

High mountain regions have undergone drastic environmental changes as a consequence of global warming during the past decades (Hock et al., 2019). The main reason for this is that the warming causes rapid melting of the cryosphere (snow and ice), which is an integral part of the mountain system (Yao et al., 2022). However, climate change impacts on mountain environments are not limited to the depletion of snow, glaciers, and permafrost. They can be observed in nearly all components of the climate system and comprise changes in vegetation cover, soil and atmospheric moisture, evapotranspiration, surface winds, river runoff, and lake levels, as well as changes in precipitation seasonality, frequency, and intensity (Hock et al., 2019).

The decline of glaciers, low-elevation snow cover, and permafrost have direct implications for the biological and hydrological systems of mountains. For example, the magnitude and seasonality of river runoff in snow-dominated and glacier-fed river basins have been significantly affected (Hock et al., 2019). Furthermore, changes in river systems and other surface waters will continue and climate model projections suggest that most of the glacier mass in mountain regions in the Middle East, Central Europe, North America, and Asia will be reduced by at least half toward the end of the century, even in a low-emission scenario (Hock et al., 2019). However, the impacts of climate change on river runoff depend on the region and are still difficult to assess on a basin scale. In some basins, river runoff is strongly dominated by the variability and changes in precipitation in the upstream regions rather than by glacier loss (e.g. Fan et al., 2022). This suggests that precipitation changes are an additional factor that will influence the regional-scale effects of climate change on river runoff.

The reason why the climate changes more rapidly in mountain regions is that the melting cryosphere triggers multiple feedback mechanisms that can enhance the warming and affect other climate components. This phenomenon is referred to as *elevation-dependent warming* (Pepin et al., 2015). Given that the widespread cryosphere and low temperatures at higher altitudes are two climate features that mountain regions have in common with Arctic regions, the idea is that some of the feedback mechanisms that lead to *Arctic amplification* (the faster increase of surface temperatures at the North Pole) also play a role in mountain regions. Such processes include but are not limited to the snow-ice-albedo feedback and nonlinear responses of temperature to increases in atmospheric moisture (i.e. cloud-related feedback effects; Hock et al., 2019). In fact, observations have shown that the Tibetan Plateau warms faster than other regions over land (Pepin et al., 2015). However, it should be noted that such elevation dependence of warming rates varies between mountain regions. While *elevation-dependent warming* indicates that different physical mechanisms control the degree of warming at different elevation bands in some regions, it does not imply that higher elevations per se exhibit higher warming rates (Hock et al., 2019).

1.1.2 Climate change impacts

The high vulnerability of mountain regions is not primarily attributed to the faster increase in surface temperatures, but rather to the multitude of risks associated with the climatic changes. Even when mountain regions are affected by the same warming rates as other terrestrial regions, this warming leads to more drastic and far-reaching impacts. Compared to other terrestrial ecosystems, mountain regions tend to be more adversely affected by and less able to recover from climate change (Hock et al., 2019). This leads to a destabilization of mountain ecosystems which has severe implications for society because they serve as a resource for land (e.g., grazing; Ehlers et al., 2022) and water (Immerzeel et al., 2020). About 10 % of the world population lives in mountain regions and is thus directly affected by the environmental and climatic changes of mountain systems (Hock et al., 2019). In addition, more than twice as many people are dependent on water from mountains (Immerzeel et al., 2020). Hence, climate change impacts on water availability and quality are not only important for local mountain communities, but also for the typically more densely populated downstream regions such as the river basins south of the Himalayas or around the tropical Andes.

The Intergovernmental Panel of Climate Change (IPCC) states that glacier melting and precipitation increases will lead to a general increase in river runoff in the near future, but to a significant decrease in river runoff in the long-term future (Hock et al., 2019). The implied water shortage in the long-term future poses a severe threat to society that is aggravated by an increasing water demand (Immerzeel et al., 2020). Some river basins in South America and Asia are, for instance, extremely vulnerable due to the steadily increasing population (Immerzeel et al., 2020). It is estimated that nearly two billion people in and around mountain regions will be negatively affected by the combined effects of water stress from climate change and increasing water demand (Immerzeel et al., 2020).

While water availability is a question that becomes particularly important on longer time scales, there are also more acute climate change impacts caused by glacier retreat and water cycle changes. The IPCC has concluded with *high confidence* that the declining cryosphere in mountain regions has led and will lead to changes in the frequency, magnitude, and location of extreme events and associated natural hazards (Hock et al., 2019). For example, landslides, avalanches, and floods can be triggered by slope instability due to permafrost thaw and shifts in seasonal snowmelt. The timing of snowmelt also influences the occurrence of wildfires. In the Rocky Mountains, wildfires have significantly increased in the past four decades due to earlier snowmelt and high spring and summer temperatures (Westerling, 2016). Moreover, the co-occurrence of early snowmelt and heavy rainfall (*rain-on-snow events*) and the associated flood risk will increase in many mountain regions as precipitation will be more likely to occur as rain instead of snow (e.g. Musselman et al., 2018). All of these hazards can cause considerable economic damage (Smith et al., 2020) and pose a severe threat to infrastructure, homes, and lives (Pörtner et al., 2022). On top of that, the exposure to natural hazards increases due to rising population density, tourism activities, and socioeconomic development in many mountain and downstream regions (Hock et al., 2019).

In summary, climate change in mountain regions is multi-faceted and involves many components of the climate system with far-reaching societal impacts (Hock et al., 2019). The severity of these impacts does not only depend on physical aspects, but also on increasing water demand, exposure, and human intervention. However, there are still many unknowns in the physical driving and feedback mechanisms of climate change in mountain regions which limits our current capability to predict impacts. A better understanding of climate processes is, therefore, critical for *climate adaption* and *societal resilience* (Pörtner et al., 2022).

1.2 Precipitation in a changing climate

Previous climate research in mountain regions has with good reason focused on glacier and permafrost loss, but the melting cryosphere is not the only driver for environmental and climatic changes. Atmospheric drivers such as water vapor transport and precipitation are key processes that have the potential to substantially affect future water availability (e.g. through changes in seasonal precipitation and evaporation) and risks for natural hazards (e.g. through rain-induced flooding). As precipitation in mountain regions is the central topic of this dissertation, this section briefly summarizes what we know about the climate change effects on precipitation globally and what implications these effects have for mountain regions.

1.2.1 Global changes

The increase in global mean temperatures triggers multiple mechanisms that affect total and extreme precipitation. One of the most important effects of global warming on precipitation is that increasing air temperatures lead to increased moisture due to the greater water-holding capacity of warm air compared to relatively colder air. This thermodynamic relationship implies that atmospheric water vapor increases with about 7 % per degree temperature increase. However, the global water and energy cycles are closely linked and dependent on each other. The global increase of precipitation is, therefore, constrained by the energy balance of the Earth system. More specifically, outgoing longwave radiation at the top of the atmosphere must be balanced by surface sensible heat fluxes and heat release from precipitation. This limits the global increase of precipitation to a rate that is only around $3\,\%\mathrm{K}^{-1}$ (Allen & Ingram, 2002; O'Gorman et al., 2012).

A global increase in atmospheric water vapor implies an increase of precipitation in regions with a net influx of moisture ("wet-gets-wetter") and a decrease of precipitation in regions with a net outflux of moisture ("dry-gets-drier"). While some regions in the world seem to roughly follow the wet-gets-wetter and dry-gets-drier trend, this rationale cannot explain all of the observed and predicted precipitation changes (Douville et al., 2021). The changing dynamics of the large-scale atmospheric circulation, changes in storm formation, and microphysical processes are important factors that need to be considered in future projections of precipitation.

1.2.2 Changes in mountain regions

Because all of the above-named factors come together on a regional scale, future projections of precipitation remain challenging, especially in regions where the mechanisms for precipitation formation at different scales are not well understood. In mountain regions, past precipitation changes have been particularly heterogeneous, partly due to decadal variability and varying large-scale circulation changes (Douville et al., 2021), but also due to the high local variability in mountain precipitation (see Chapter 2.2.3). Hence, there are no consistent trends in annual precipitation, but most mountain regions show a significant decrease in the relative contribution of snowfall to total precipitation (Douville et al., 2021). Global climate model projections suggest that precipitation will increase in the order of 5 % to 20 % over the tropical Andes, the Hindu Kush Himalayas, East Asia, East Africa as well as the Carpathian region, while it will decrease in the Southern Andes and Mediterranean region (Hock et al., 2019). Some regions such as the Himalayas and the Tibetan Plateau show also a future increase in the intensity and frequency of extreme precipitation (Hock et al., 2019). However, global and regional climate model simulations do not always show the same climate signal and the magnitude in trends (e.g. Gao et al., 2018). The question as to what drives total and extreme precipitation changes in different mountain regions of the world is therefore still not solved.

1.2.3 Predicting precipitation changes

A major uncertainty in future projections of precipitation changes is that conventional global and regional climate models cannot resolve all the processes that form precipitation. Convective precipitation, i.e. precipitation that occurs due to convective lifting at scales below the resolution of global climate models, has to be represented using empirical relationships, so-called parametrizations. This means that conventional climate model projections treat important processes that affect the spatial distribution, intensity, and frequency of precipitation only approximately. Non-hydrostatic kilometer-scale (hereafter: km-scale) climate simulations are a promising solution to uncertainties in convective parameterization, as they realistically resolve large storms (Prein et al., 2021). Because km-scale climate simulations have the potential to provide new insights into regional-scale precipitation processes, they are an important topic of this dissertation that is addressed in more detail in section 3.4.

1.3 The Tibetan Plateau and its downstream regions

1.3.1 Importance for water resources and climate change context

The Tibetan Plateau (hereafter: TP) and its surrounding mountain ranges are together the largest and highest mountain region in the world. The TP is often nicknamed *"Asia's water tower"* or the *"Third Pole"* to highlight the region's similarity to polar climate regions and its importance for water resources. In fact, the TP is the third largest freshwater storage after the Arctic and Antarctica. The TP is the headwater of many major river systems in Southeast Asia, e.g. the Indus, Ganges-Brahmaputra, Mekong, Yangtze, and Yellow river (Fig. 1.1), some of which are ranked as the most vulnerable river systems to climate change on Earth (Immerzeel et al., 2020).

The region has experienced warming that is twice as fast as the global average (Yao et al., 2022) and many of the climatic changes summarized in section 1.1 have been observed in the TP region (Bibi et al., 2018; Ehlers et al., 2022). In particular, it has been found that there is an overall wetting and acceleration of the water cycle over the TP (Bibi et al., 2018). However, there is a lack of understanding of what this implies for sub-regional precipitation changes and which atmospheric processes will dominate future changes in precipitation.

1.3.2 Large-scale atmospheric systems affecting precipitation the TP region

The TP has a dry, tundra-like climate, whereas its surrounding lower-elevation river basins are temperate to tropical. Despite this difference in climate regimes, both regions are characterized by a distinct wet and dry season controlled by the *South Asian summer monsoon*. The South Asian summer monsoon describes the seasonal reversal in the prevailing large-scale wind circulation with more southerly winds during summer that transport warm and humid air from the maritime regions to the land. The associated enhanced water vapor transport from the ocean influences the seasonal cycle of precipitation over land. Figure 1.2 visualizes the linkage between atmospheric water vapor transport and the distribution of precipitation over East Asia. Between May and September, the enhanced atmospheric water

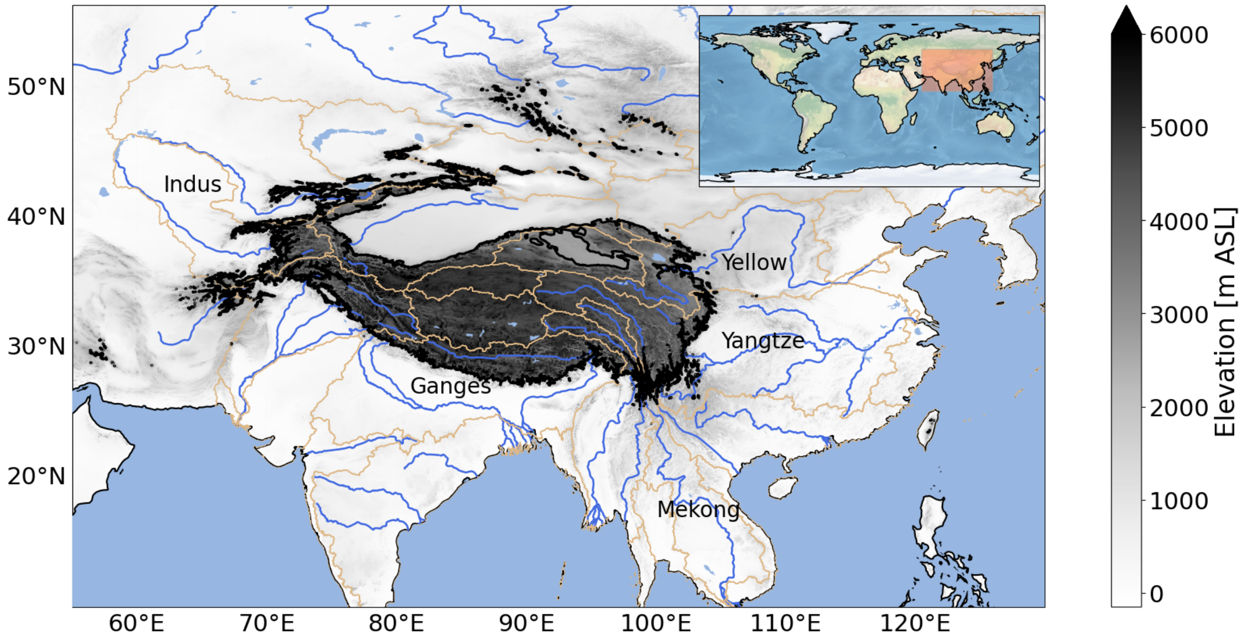

Figure 1.1: The Tibetan Plateau with its major river systems and surrounding basins. The color shading shows the elevation obtained from the Shuttle Radar Topography Mission (Farr et al., 2007) and the orange contours depict the boundaries of the major river basins derived from the HydroSheds database (Lehner & Grill, 2013). The black contour indicates the 3000 m ASL (above sea level) boundary of the TP.

vapor transport is associated with a significant increase of precipitation over ocean and land (Fig. 1.2).

Another important large-scale atmospheric system that influences the climate in the TP region is the *extra-tropical westerly circulation*. Driven by pressure differences between subtropical and sub-polar regions, the westerlies are the prevailing winds in the upper troposphere of the mid-latitudes. Figure 1.3 shows the seasonal migration of westerlies over the TP region. The westerlies are stronger and closer to the equator during winter, whereas they weaken and move northward during the summer. A particularly important feature embedded in this circulation is the westerly jet stream that describes the core region of maximum wind speeds (Schiemann et al., 2009). Figure 1.3 shows that this core region, in which winds exceed $20\,\mathrm{m\,s^{-1}}$, is located at the southern edge of the TP during winter and propagates to the northern edge over the TP during the summer months. The westerly jet has been widely recognized to interact with the monsoon circulation and the topography of the TP, thereby influencing the weather in the downstream regions (Schiemann et al., 2009). Isotope analyses suggest that water vapor for precipitation formation over the northern TP originates from the transport through westerlies whereas the water vapor for precipitation in the southern TP originates from the transport through the monsoon circulation (Yao et al., 2013). However, the effects of the westerly jet on regional precipitation are more generally indirect and unexplored compared to the effects of the monsoon circulation.

Owing to its immense height and extent, the TP interacts with the large-scale atmospheric circulation and shapes the climate over East Asia in multiple ways. For example, it is regarded as an important factor in the onset of the Asian summer monsoon by acting as a major heat source during summer (Flohn, 1957; Ye & Wu, 1998). On a more regional scale, it influences the weather and climate in the downstream regions when mountainous weather systems are transported eastward with the prevailing westerly circulation (e.g. Curio et al.,

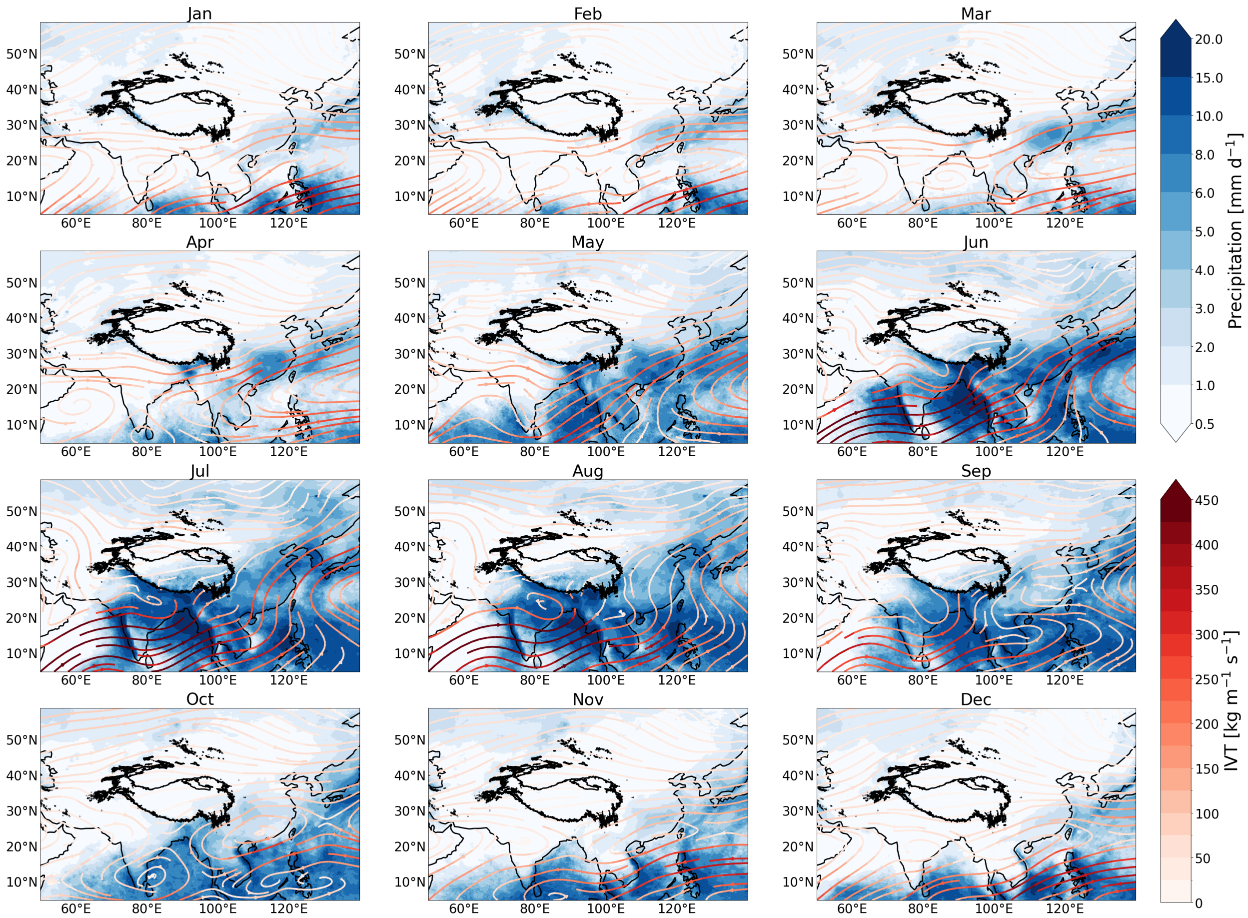

Figure 1.2: Large-scale atmospheric circulation systems affecting the TP region: The Asian summer monsoon, visualized as the monthly evolution of mean surface precipitation (color shading) and the monthly evolution of the mean water vapor fluxes (streamlines). The monthly surface precipitation has been derived from GPM IMERG for 2000–2021 and the water vapor fluxes have been derived from the ERA5 reanalysis for 1979–2019. The colors of the streamlines indicate the magnitude of the total vertically integrated water vapor transport IVT= $\int \sqrt{qu^2 + qv^2}$, where qu and qv represent the eastward and northward components of horizontal water vapor fluxes.

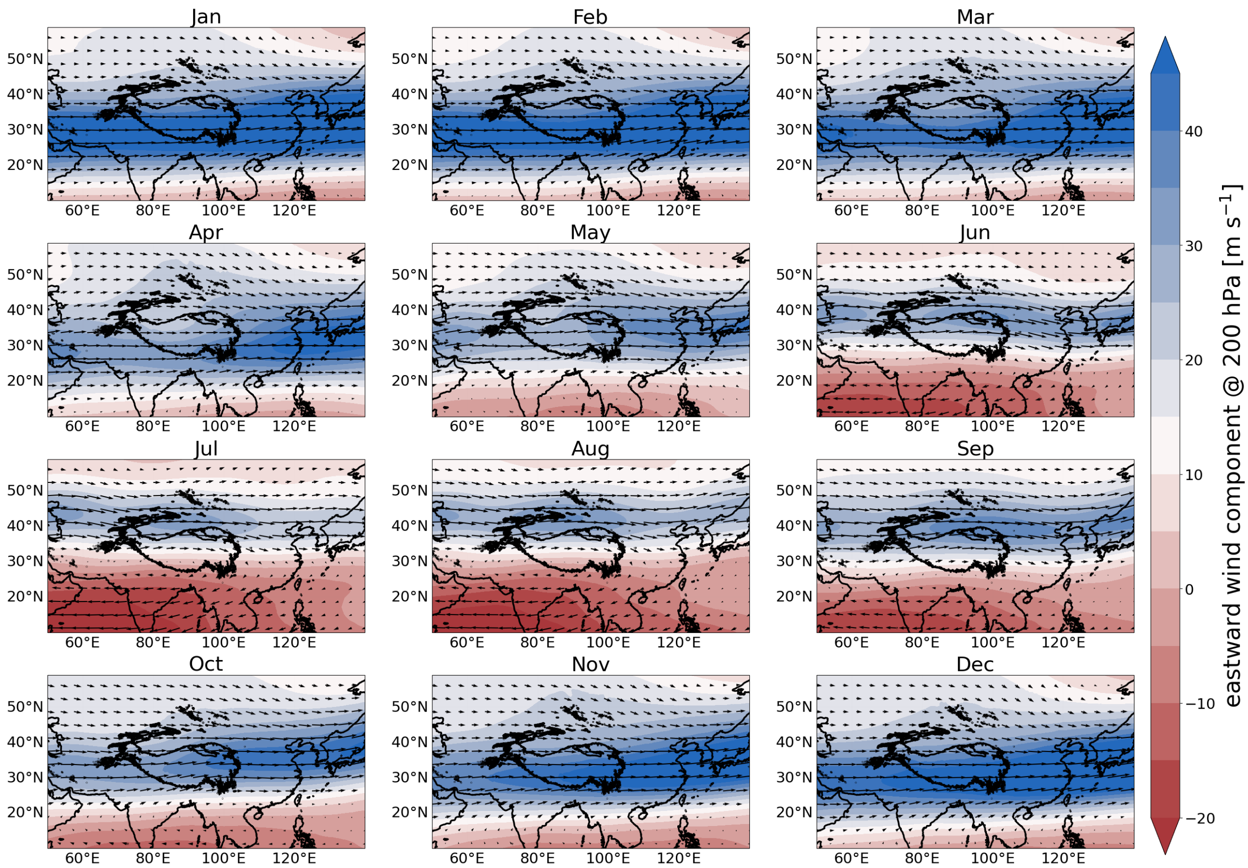

Figure 1.3: Large-scale atmospheric circulation systems affecting the TP region: The westerly circulation, visualized as the monthly evolution of mean zonal wind at 200 hPa, derived from the ERA5 reanalysis for the time period 1979–2019. The location of the westerly jet stream corresponds approximately to the maximum in the zonal wind speed at 200 hPa

2019). In this dissertation, precipitation processes are therefore not only discussed for the TP itself but also for the regions south and east of the mountains that are directly coupled to the TP climate. The term *TP region* is used to describe the TP mountains together with its downstream regions. In contrast to that, the term *TP* is used to describe the higher mountain area, defined by the 3000 m elevation boundary shown in Figure 1.1. Note that no clear boundary is defined for the *TP region*, as the impact of the TP on its downstream regions varies with the context of the appended papers.

1.3.3 Regional climate processes

Unlike what the name "plateau" suggests, the TP is not just an elevated area. Instead, it is characterized by high variations in topography with many mountain tops exceeding the average elevation of around 4000 m. The complex topography makes it difficult to observe and model the regional climate of the TP because it implies a high local variability in meteorological parameters, heterogeneous surface types, and various different small-scale processes influencing the weather and climate.

Convective precipitation represents one of the climate components that is not well understood, even though it has long been recognized that mountain convection over the TP is an important process for the regional climate (Flohn & Reiter, 1968; Yeh, 1982). While convective precipitation can be related to small-scale processes, it can also occur in the form of large convective storms. A particularly large type of convective storms, so-called *mesoscale convective systems (MCSs)*, has been recognized as a prolific rain-producer affecting the TP and its downstream regions. Figure 1.4 shows an example of satellite observations of an MCS producing heavy rainfall at the eastern edge of the TP. Even though MCSs are clearly observable in satellite observations, their more detailed features, their importance for seasonal and extreme precipitation, and their underlying mechanisms remain largely unexplored. In this dissertation, MCSs are investigated as an additional mechanism that affects regional precipitation patterns and interacts with the large-scale atmospheric circulation.

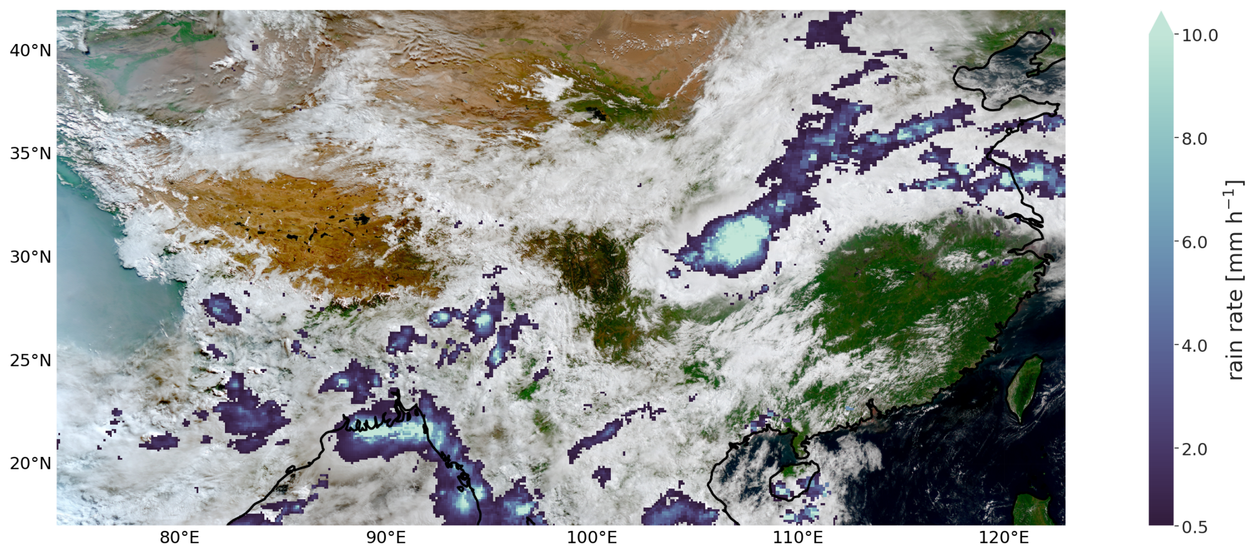

Figure 1.4: Example of a large storm system (mesoscale convective system) in July 2020 on the downwind side of the TP (∼105°E) as seen from satellite observations. The figure shows a true color image from the satellite Himawari (Bessho et al., 2016) overlayed by rain rates estimated from GPM IMERG. The satellite observations reveal also multiple other storm systems over the ocean which are characterized by cloudy areas and high rain rates. The black contour depicts the coastline.

1.4 Objectives and structure

Despite the scientific and societal relevance of precipitation, it remains one of the least understood components of the climate system of mountain regions. Therefore, the overarching aim of this dissertation is to **advance the understanding of present-climate precipitation characteristics and its underlying large-scale and mesoscale processes in the Tibetan Plateau region**. A particular focus is the role of convective storms in the water cycle over the TP and its downstream regions.

The more specific objectives are:

1. To identify major **large-scale atmospheric processes and systems** that govern the spatiotemporal distribution of precipitation and convection (**Paper I**, **II**, **III**, **VI**)
2. To investigate the importance of **mesoscale convective systems** for precipitation and to investigate their spatial and temporal characteristics (e.g. lifecycle, size, duration) at the storm scale (**Paper IV**, **V**, **VII**)
3. To evaluate how well large-scale atmospheric processes, mesoscale convective systems, and their impact on precipitation are represented in **kilometer-scale model simulations** (**Paper V**, **VI**)

To achieve these objectives, cloud and precipitation characteristics are presented from multiple perspectives, including sub-seasonal to decadal scales and sub-regional to regional scales. In addition, this research combines information from multiple data sources, namely gauge measurements, satellite observations, reanalysis data, and state-of-the-art numerical weather and climate model simulations.

The remainder of this dissertation is structured as follows: Chapter 2 provides a background on processes at different meteorological scales that influence precipitation in general and over mountain regions in particular. Chapter 3 explains methods to observe and model mountain precipitation and related challenges. Chapter 4 highlights the key results obtained from the scientific papers of this dissertation. Chapter 5 summarizes the main conclusions by referring back to the above-listed objectives. Chapter 6 discusses these conclusions in a broader context and provides ideas for future research paths.

Chapter 2

PRECIPITATION PROCESSES

Precipitation refers to hydrometeors, i.e. water and ice particles, that form in the atmosphere and grow large enough to fall down. The formation and growth of hydrometeors involve microphysical processes that occur at scales from micro- to centimeters (Lohmann et al., 2016). These processes are largely dependent on the particle phase and concentration of hydrometeors and determine how efficiently precipitation is produced (Lohmann et al., 2016). The environment in which these processes occur is, in turn, determined by atmospheric dynamics, which are the focus of this dissertation.

This chapter describes different atmospheric processes that influence the regional distribution as well as large- and mesoscale structures of precipitation. The chapter starts by discussing the role of atmospheric water vapor transport and atmospheric convection as two vital processes for precipitation formation over land. The second part of this chapter focuses on specific mechanisms that are relevant for precipitation formation in mountain regions.

2.1 General precipitation processes

2.1.1 Definition of scales

Although atmospheric processes occur on a continuous spectrum of sizes, it is common to classify them into different spatial scales. These scales represent peaks in the spectral density of atmospheric motion (e.g. visible in frequency spectra of zonal kinetic energy; Trapp 2013) and facilitate the discussion of processes influencing precipitation variability. The two major scales of interest in this dissertation are the **large-scale** and **mesoscale**. Following the classification proposed by Orlanski (1975), these scales are defined as:

Large-scale refers to horizontal scales >2000 km and involves processes occurring over multiple days to months.

Mesoscale refers to horizontal scales between 2 km and 2000 km and involves processes that last from a few hours to days.

Note that we use a third scale in this particular chapter to describe **local processes** in mountain regions. These overlap partly with mesoscale processes, but occur usually at smaller scales and are not the main focus of this dissertation.

2.1.2 The atmospheric water cycle and water vapor transport

The Earth's water cycle describes how water in its various forms (i.e. vapor, liquid, or frozen) is stored and transported in the climate system (Fig. 2.1). Precipitation is one component in this cycle and the principal flux from the atmosphere to soils, surface waters, and the ocean. While precipitation removes water from the atmosphere, the addition of water to the atmosphere at a certain location is controlled by either local surface evaporation or atmospheric water vapor transport into the region. Atmospheric water vapor transport is especially important for precipitation over land, where evaporation is significantly smaller than over the oceans.

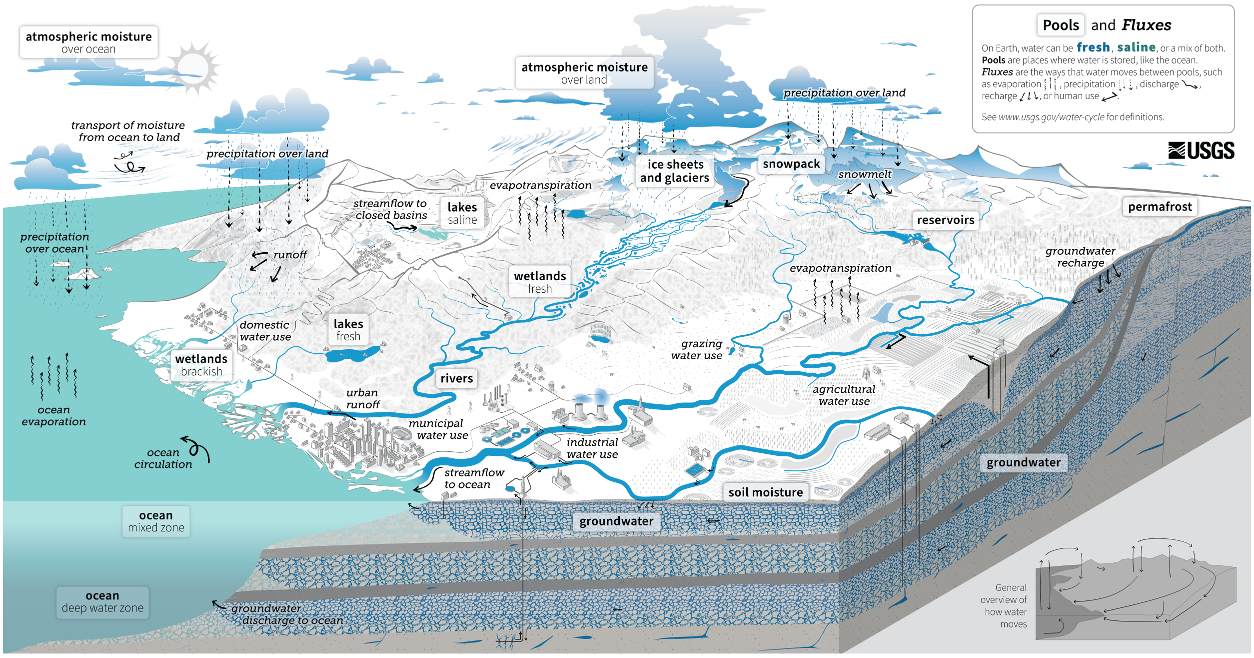

Figure 2.1: The Earth's water cycle with its pools (boxes) and fluxes (italic text) of water. Source/Usage: Public domain. The figure is provided by the US Geological Survey and can be downloaded from https://www.usgs.gov/special-topics/water-science-school/science/water-cycle.

Because the amount of water that is stored in any component of the water cycle (the *pools* in Fig. 2.1) is approximately constant, the fluxes between them have to be in balance. For the atmospheric branch of the water cycle, this means that precipitation is balanced by evaporation and atmospheric water vapor transport. Hence, the amount of precipitation at a certain location averaged over a longer time period (e.g. seasonal mean) should approximately correspond to the sum of evaporation and the degree to which water vapor is converging into the region (Peixoto & Oort, 1992). The local net influx of water vapor can be quantified using the *horizontal moisture flux convergence*. Mathematically, the balance between precipitation, evaporation, and net water vapor influx can be described as:

$$\overline{P} - \overline{E} \approx \underbrace{\overline{-\nabla \int_{p_s}^{p_t} (q\overrightarrow{V})dp}}_{\text{horizontal moisture flux convergence}} \tag{2.1}$$

where $\overline{P}$ is the temporal mean of precipitation, $\overline{E}$ the temporal mean of evaporation (Peixoto

& Oort, 1992). The right-hand side of the equation is the negative divergence (hence: convergence) of the horizontal moisture fluxes integrated over pressure levels with q referring to specific humidity and $\overrightarrow{V}$ referring to the horizontal wind vector.

Figure 2.2 shows that the summer mean of *horizontal moisture flux convergence* ($\nabla \int_{p_s}^{p_t} \overline{qV}$) over the TP region is balanced by the summer mean precipitation ($\overline{P}$) minus the summer mean evaporation ($\overline{E}$). This demonstrates that precipitation is directly coupled to atmospheric water vapor transport and highlights the importance of large-scale atmospheric circulation systems that control atmospheric water vapor transport in specific regions and seasons.

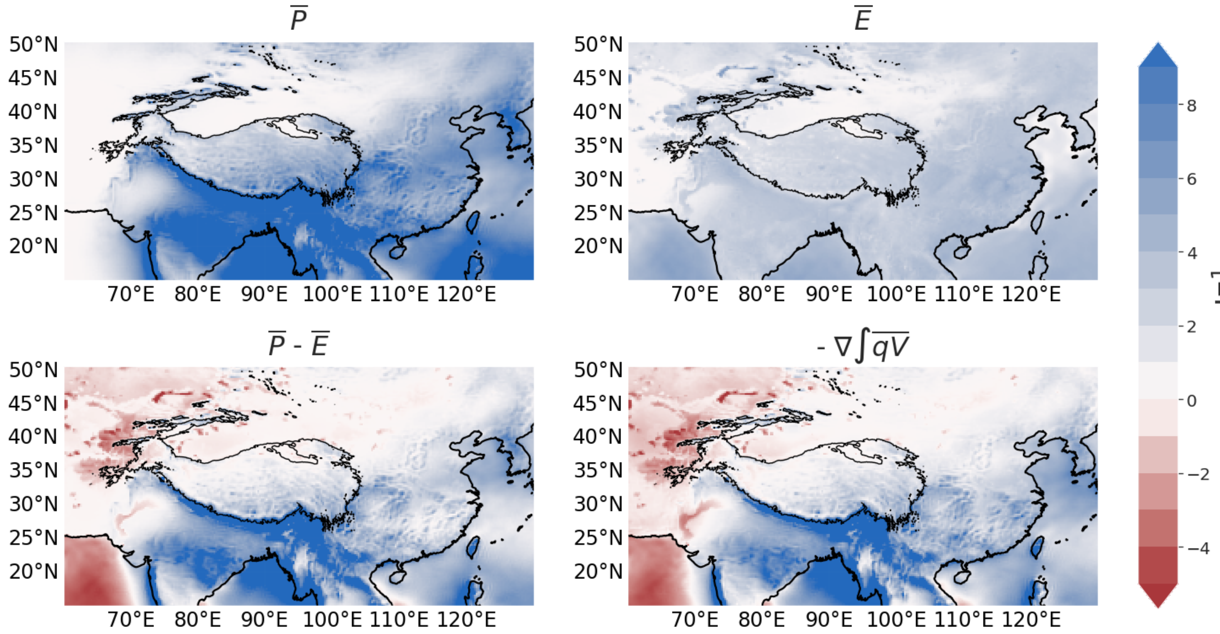

Figure 2.2: Components of the atmospheric water cycle for the TP region showing mean summer precipitation ($\overline{P}$), mean summer evaporation ($\overline{E}$) and horizontal moisture flux convergence ($\nabla \int_{p_s}^{p_t} \overline{qV}$, where q refers to specific humidity and V to the wind vector) integrated from surface pressure (p_s) to top pressure (p_t). The means have been calculated based on monthly means from ERA5 for June–August 1980–2019 (Figure modified from **Paper 7**).

2.1.3 Atmospheric convection

Atmospheric convection is a precipitation process occurring at the mesoscale or smaller. It works similarly to convection in a pot of cooking water: Some regions in the fluid are heated greater than others, which causes these hotter and less dense regions to rise while the colder and more dense regions sink. In the atmosphere, this heat transfer results from surface heating by the sun or from mechanically forced upward motion by wind circulation, topographic barriers, or friction. Atmospheric convection plays a key role in the global water and energy cycle because it redistributes heat and moisture between the surface and the upper levels of the troposphere. In the presence of water vapor, convection leads to the formation of clouds, which makes it a key mechanism for precipitation formation.

This is particularly true for *convective precipitation* which refers to short-term heavy precipitation that forms in updrafts. *Convective precipitation* is usually distinguished from the more moderate *stratiform precipitation* that is associated with large-scale lifting. Due to different mechanisms involved in the formation of *stratiform* and *convective precipitation*, these two types of precipitation are affected differently by climate change. For example, *stratiform precipitation* is estimated to increase with only $1\%\,K^{-1}$ to $3\%\,K^{-1}$ (O'Gorman, 2015), while orographic and *convective precipitation* are expected to increase at rates higher than the estimated increase of atmospheric water vapor of $7\%\,K^{-1}$ (e.g. Berg et al., 2013; Lenderink et al., 2017). However, convection as a process is still relevant in the formation of both types of precipitation because they often occur in the same convectively driven storm system (Houze Jr, 1997).

The *organization of convection* into storms is a somewhat loosely defined concept that can involve many different physical mechanisms. It helps, however, to distinguish long-lived clusters of convective clouds and well-organized storm systems from isolated convection. Isolated and scattered convection is different from *organized convection* because it occurs more randomly in time and space. It is sometimes also referred to as *popcorn convection*, simply because it pops up quickly (e.g. as a consequence of surface heating) and disappears after a short time. In contrast to this short-lived occurrence of convection, *organized convective storms* generate an internal circulation that helps the storm system aggregate several convective cells and maintain itself for several hours or days.

Although convective storms exist on a wide spectrum of different temporal and spatial scales, they are characterized by relatively large vertical and horizontal extents as well as a longer duration compared to isolated convection. This implies that they produce large precipitation volumes during their lifetime. In contrast to the relatively harmless nature of isolated convection, organized convective storms can be severe, especially when their strong winds and large amounts of heavy precipitation affect the same area for several hours. The changing degree of convective organization (Pendergrass, 2020) and the intensification of future storms over some regions (e.g. Prein, Liu, Ikeda, et al., 2017) are important drivers for future changes in extreme precipitation. However, convective storms are not only responsible for precipitation extremes but also contribute significantly to the total seasonal precipitation in some regions, as will be demonstrated in more detail in Chapter 4.2.1. This is particularly true for *mesoscale convective systems (MCSs)*, one of the largest forms of organized convection. Since MCSs are a central topic of this dissertation (see Objective 2), the next section will introduce this specific storm type in more detail.

2.1.4 Mesoscale convective systems

Mesoscale convective systems (MCSs) are complexes of storms with horizontal dimensions that span over several hundred to thousands of kilometers (Houze Jr, 2004). They are important rainfall producers in the tropics and midlatitudes, which is why agriculture in some regions depends on the occurrence of these storm systems. At the same time, MCSs can cause destructive hazards and deaths, for example when they produce large hail or trigger flash floods (Schumacher & Rasmussen, 2020). Over land, MCSs are most common in the tropics and in the baroclinic zones downwind of major mountain ranges in the mid-latitudes (Feng et al., 2021).

While the exact definition of the size of MCSs varies in the literature, they usually produce precipitation over an axis of at least 100 km and persist for at least three hours in the mid-latitudes (Houze Jr, 2004). Typically, MCSs are characterized by larger areas of *stratiform precipitation* behind or surrounding the smaller region of *convective precipitation* (Houze Jr, 2004). These features make MCSs easily observable from space because the convective part appears particularly bright in visible and cold in infrared (IR) satellite imagery owing to the high reflectivity and low cloud top temperature of deep convective clouds (Fig. 2.3).

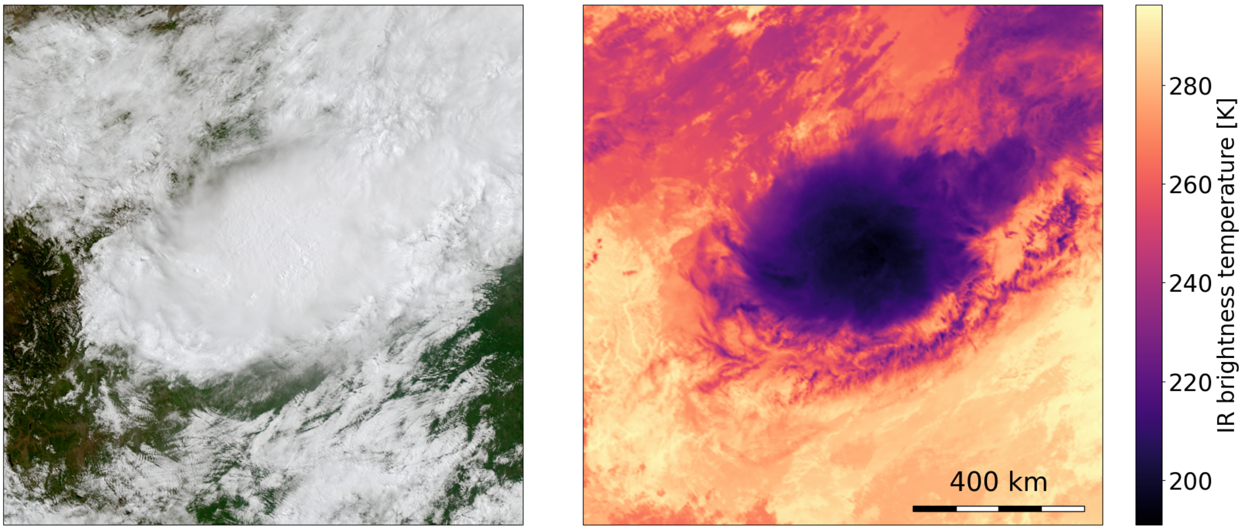

Figure 2.3: Example image of an MCS occurring at the eastern edge of the TP (July 2020) seen from space in a true color image (left) and infrared (IR) image (right). The MCS appears bright in the true color image due to the high reflectivity of deep clouds. Because the measured emission in the IR image stems from the cloud top, deep clouds appear cold in the IR image. The images were derived from the satellite Himawari (Bessho et al., 2016).

The key ingredients for MCS formation are moisture supply, uplift, and atmospheric instability. However, their growth may be controlled by different physical mechanisms, e.g. interaction with the large-scale circulation and interaction between *cold pools* (cold air masses) and convective updrafts (Schumacher & Rasmussen, 2020). Because all of these ingredients are likely to be affected by climate change, the distribution and properties of MCSs will change in the future. How exactly these changes look in specific regions is a relatively new research topic that is currently getting increasing attention due to the ability of high-resolution climate models to better represent MCS dynamics (Schumacher & Rasmussen, 2020).

2.2 Precipitation processes in mountain regions

Mountain regions play a key role in forming mid-latitude weather due to the mechanical and thermodynamic effects of orography on wind circulation and energy fluxes. Despite the lack of observations in mountain environments, there is a lot of theoretical knowledge about the effects of mountains on air motion and other atmospheric variables, e.g. from idealized model simulations and climate model experiments wherein mountains have been removed (Barry, 1992). The interactions between mountains and the above-lying atmosphere take place at different spatial scales which means that precipitation formation is influenced in various ways (Barry, 1992).

2.2.1 Large-scale processes

Extensive mountain regions like the Andes, the Rocky Mountains, the TP, and the Himalayas influence the global climate system through the generation of planetary-scale or gravity waves and through the dynamical modifications of the large-scale circulation (Barry, 1992).

Dynamical modification in this context means that the prevailing wind circulation can be blocked or deflected by the mountain barrier. For example, the extratropical westerlies are split at the lower levels of the troposphere when they encounter the Rocky Mountains in North America or the TP in East Asia (Barry, 1992). Another example is the barrier effect of the Himalayas which prevents the moist and warm summer monsoon air masses from propagating further north (this effect can for example be seen in Fig. 1.2 in section 1.3.2). The dynamic modification of the wind circulation and the generation of wave patterns have, in turn, far-reaching impacts on the continental precipitation distribution that are not limited to the mountain region itself. For instance, global climate model experiments without mountains show that high-altitude regions such as the TP and Colorado plateaus are needed to create monsoon-like circulations around them. Without the mountains, the climate in Northwest America and Central Asia would be moister while East Asia would be substantially drier (Barry, 1992).

Owing to their height and large spatial extent, major mountain regions represent large-scale heat sources that warm the middle and upper troposphere. For example, the role of the TP as an elevated heat source has long been recognized and discussed as a crucial factor influencing the large-scale atmospheric circulation during summer (Flohn, 1957). While the heating of elevated surfaces occurs over relatively large scales, the resulting convection can be very localized. The formation of convective clouds due to intense surface heating during summer is a common phenomenon in many mountain regions (Barry, 1992). Surface heating and heat release from precipitating clouds can also change the properties of weather systems such as fronts passing the mountains, e.g. by altering temperature and pressure gradients (Barry, 1992).

Because mountain regions are usually moisture-limited environments, the large-scale advection of atmospheric water vapor from remote regions is an important factor controlling how much moisture is available in and around the mountains. As was shown in Figure 1.2, the water vapor supply in the TP region is largely influenced by the monsoon circulation that transports water vapor from the maritime regions in the south towards the inland during summer. Around the Rocky Mountains and Andes, there are similar circulations and it has been shown that the low-level jets associated with these circulations provide moisture that is needed for convective storm formation in the lee of major mountains (e.g. Rasmussen & Houze Jr, 2016). **Paper V** and **Paper VI** investigate in more detail what role moisture transport from remote regions plays for convection in the lee of the TP.

2.2.2 Mesoscale processes

Lee cyclogenesis refers to the formation of cyclones at the downwind side of mountains and is common where major mountain ranges interact with the mid-latitude westerly circulation. Therefore, the Rocky Mountains, the TP, and the European Alps stand out as major centers for cyclogenesis in the northern hemisphere during winter (Barry, 1992). There are multiple mechanisms involved in the generation of lee cyclones, e.g. the warming of descending air on the downslope in the case of the Rocky Mountains. From a dynamical point of view, the generation of cyclonic rotation is mainly due to the vertical stretching of the air column on the lee side of the mountains. Since the relationship between the sum of relative vorticity (degree of rotation) and planetary vorticity (Coriolis parameter) in relation to column thickness needs to be constant, an increase in column thickness implies that either the planetary or relative vorticity (hence: cyclonic rotation) needs to increase. When *lee cyclogenesis* occurs during the boreal summer season in the northern hemisphere (boreal winter season in the southern hemisphere), it is often related to convection (e.g. Rasmussen & Houze Jr, 2016).

In addition, downwind regions can be affected by *capping inversions* when the relatively warmer and drier air from the mountains lies above the moister and colder air on the downwind side. Such stable conditions prevent the release of instability and lead to the accumulation of energy. Eventually, the uplift of moist air in these regions manages to break through this *capping inversion* and triggers severe convection. This mechanism has been found to frequently occur in the lee of the Rocky Mountains (Carlson et al., 1983) and subtropical Andes (Rasmussen & Houze, 2011).

Further, mesoscale disturbances might form over the mountains as a consequence of modifications of the large-scale circulation (see previous section) or diabatic heating. For example, *Tibetan Plateau vortices* (TPVs; Curio et al., 2019) are frequently occurring mesoscale cyclonic low-pressure systems that form over the northwestern TP and propagate eastward with the prevailing westerly circulation (Fig. 1.3). Figure 2.4 shows an example of a TPV forming over the central northern TP during summer. TPVs can have significant effects on the downstream weather and have been associated with heavy precipitation when they enter the lower-elevated plains (Curio et al., 2019). Similar mesoscale disturbances propagating eastward over the Rocky Mountains have been linked to the initiation of summer MCSs over the Great Plains (Song et al., 2021; Wang et al., 2011). The role of TPVs in MCS formation around the TP has so far not been addressed and is analyzed for a particular MCS case in **Paper V**.

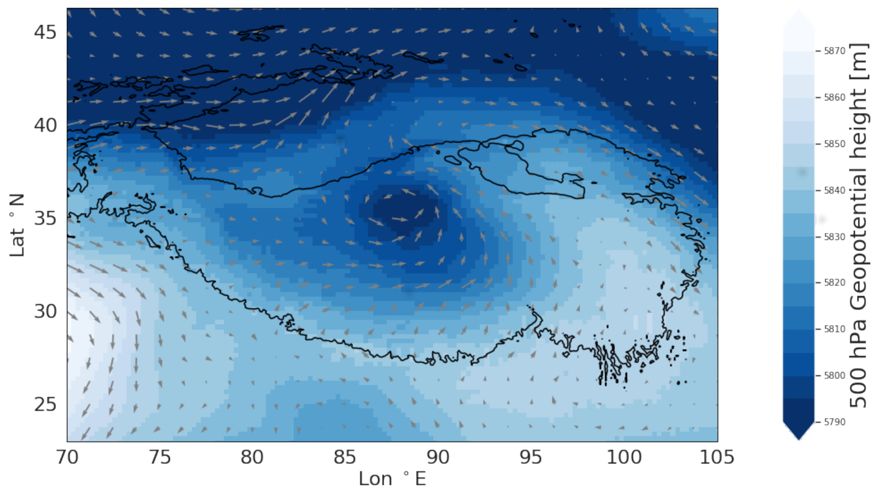

Figure 2.4: Example of a mesoscale vortex originating over the TP during summer. The vortex is featured by cyclonic rotation and a low-pressure center, here shown based on horizontal wind vectors and geopotential height at 500 hPa derived from ERA5.

2.2.3 Local processes

Mountain circulations at horizontal scales between 1 km and 100 km are important for local and short-duration precipitation (Barry, 1992). Thermally-induced slope winds (i.e. katabatic and anabatic winds) and mountain valley breezes occur due to contrasted surface heating and cooling between day and night (Barry, 1992). The resulting local atmospheric conditions eventually trigger updrafts and interact with microphysical processes that control cloud and precipitation formation at the slopes (Barry, 1992).

A widely observed phenomenon is the enhancement of precipitation by *orographic lifting*. Multiple factors, e.g. atmospheric instability and terrain steepness, can influence the uplift of air masses over mountains which consequently favors cloud formation and condensation at higher altitudes of the atmosphere (Barry, 1992). This process often interacts with other processes, so precipitation can be orographically enhanced, regardless of whether it was initially formed by a local process, in a convective storm, or in a large-scale air mass that is pushed against a mountain barrier (Barry, 1992).

Lastly, surface properties such as soil moisture and vegetation regulate heat fluxes in the boundary layer. For example, wetter soils are associated with enhanced radiative heating of the surface. This increases heat and moisture fluxes into the lower atmosphere which act as fuel for the development of convection (Trapp, 2013). Such land-atmosphere interactions and their resulting circulations can occur over larger areas and, if soil moisture is involved, give rise to feedback mechanisms with relatively slow time responses (Trapp, 2013). However, these interactions can also occur very localized, especially in mountain regions because small-scale variations in topography imply a heterogeneity in surface properties. Over the TP, it has been suggested that regions with locally higher soil moisture contents favor convective initiation (Barton et al., 2021; Sugimoto & Ueno, 2012)). In addition, other factors such as topography, winds, and vegetation have been discussed to influence local variations in convection intensity (Barton et al., 2021).

Chapter 3

OBSERVING AND MODELING MOUNTAIN PRECIPITATION AND CONVECTION

Observing and modeling clouds and precipitation in complex terrain continues to be a major challenge in atmospheric science, even though observation and modeling capabilities progressed significantly during the past two decades. This chapter presents state-of-the-art methods to observe and model mountain precipitation and convection. The main advantages and limitations of different data sources are discussed based on examples from the Tibetan Plateau region and an overview of the specific data sets, their coverage, and resolution is provided at the end of this chapter.

3.1 Ground-based observations

Put simply, rain and snow gauges are buckets that collect precipitation. They are indispensable for precipitation-related research and are usually seen as the *ground truth* for surface precipitation because they are the most direct measurements available. However, gauges measure precipitation over a very limited area, which limits their ability to capture the spatial distribution of precipitation.

Gauge networks in mountain regions are typically less dense than in easily accessible areas, simply because it is more difficult and expensive to maintain meteorological stations in remote regions and harsh environments, especially during winter. For example, most gauge stations over the TP are located in the eastern parts and below the average elevation of 4000 m ASL. Hence, there are almost no measurements of precipitation in the central and northwestern parts of the TP and the higher altitudes of the Himalayas (Fig. 3.1e).

Another limitation of gauge measurements in mountain regions is that precipitation can show large differences between valleys and mountaintops. Because mountain weather is influenced by various topography-related processes (see section 2.2.3), a particular gauge station may not be representative of a larger area. For example, a station could measure precipitation that is locally enhanced by the orography or, conversely, it could miss the orographic effects of the surroundings. In addition, the quality of gauge measurements has been shown to be significantly affected by wind-induced undercatch of snow (Groisman & Easterling, 1994) and by varying catch efficiencies of different instruments (Rasmussen et al., 2012). As a consequence of undercatch and orographic effects, global gauge measurements of precipitation show the largest biases over high mountain regions when compared to precipitation inferred from water budgets based on stream flow observations (Beck et al., 2020).

3.2 Satellite retrievals

In contrast to gauge measurements, satellite observations can provide spatially continuous estimates of precipitation, even in remote areas. Advances in remote sensing technology and new satellite missions over the last two decades (e.g., Kidd & Huffman, 2011; Stephens et al., 2002) have offered new possibilities to gain insights into cloud and precipitation processes.

There are various current and historical satellite sensors that can be used to observe clouds and precipitation. However, the aspects of clouds and precipitation that can be investigated with satellite observations depend on the characteristics of the respective sensor. *Active* satellite sensors, for example, send out beams of radiation and measure its reflection from atmospheric features. The time between the emission and reception of the reflected signal can be used to infer the vertical structure of the observed features. This is particularly useful for studying convective storms because these are characterized by clouds with deep vertical extents. However, active satellite measurements typically have a more limited temporal and spatial coverage compared to *passive* satellite sensors that measure reflected solar radiation or thermal emission from the atmosphere. For example, radar measurements from the *CloudSat* mission (Stephens et al., 2002) overpass the TP during two specific times of the day (around 1:30 am and 13:30 pm local time), limiting their ability in capturing the complete diurnal cycle of convection (**Paper I**).

Figure 3.1 illustrates what aspects of clouds and precipitation are captured by different observations based on an example case of summer convection over the TP. The uppermost panels show cloud observations seen from two different satellite sensors. Figure 3.1a shows passive measurements of thermal infrared (IR) brightness temperatures with low temperatures indicating cold (and thus high) cloud tops. The red line indicates the trajectory of an overpass of the active sensor from the CloudSat satellite mission during the same time. Figure 3.1b shows the vertical profile of clouds during that overpass, revealing several deep convective clouds during the daytime. While the observations from the top can see the complete horizontal extent of cloud systems, they provide only limited information on the vertical extent through the temperature that is linked to cloud top height. They do, however, not contain any information on the vertical structure that is instead captured by active sensors. In this dissertation, satellite observations of IR brightness temperatures have been used to identify and track MCSs (**Paper IV**, **Paper V**), whereas satellite observations from CloudSat have been used to study sub-regional differences in the distribution of clouds over the TP (**Paper I**).

Further, Figure 3.1c shows satellite-retrieved precipitation from the *Global Precipitation Measurement Mission* (GPM; Kidd & Huffman, 2011). *Satellite retrievals* are indirect measurements because they infer physical quantities such as precipitation from the electromagnetic radiation measured by the satellites. The retrieval, which involves statistical or physical modeling, introduces additional uncertainties that are particularly high in heterogeneous mountain regions like and in regions with few gauge measurements available to correct and validate retrieved precipitation. However, satellite-retrieved precipitation represents the best observations available for studying spatial patterns of precipitation at a high temporal resolution. Figure 3.1c shows, for instance, that GPM IMERG indicates precipitation occurring over the central TP that is consistent with the cloud observations (Fig. 3.1a). These precipitating areas are not captured by the gauge measurements because there are no stations located over all areas where precipitation occurs (Fig. 3.1e).

A drawback of many satellite-based precipitation data sets is that they do not reach as far back in time as gauge measurements and reanalyses (Fig. 3.1f). This makes them less useful to study decadal variability and climate trends.

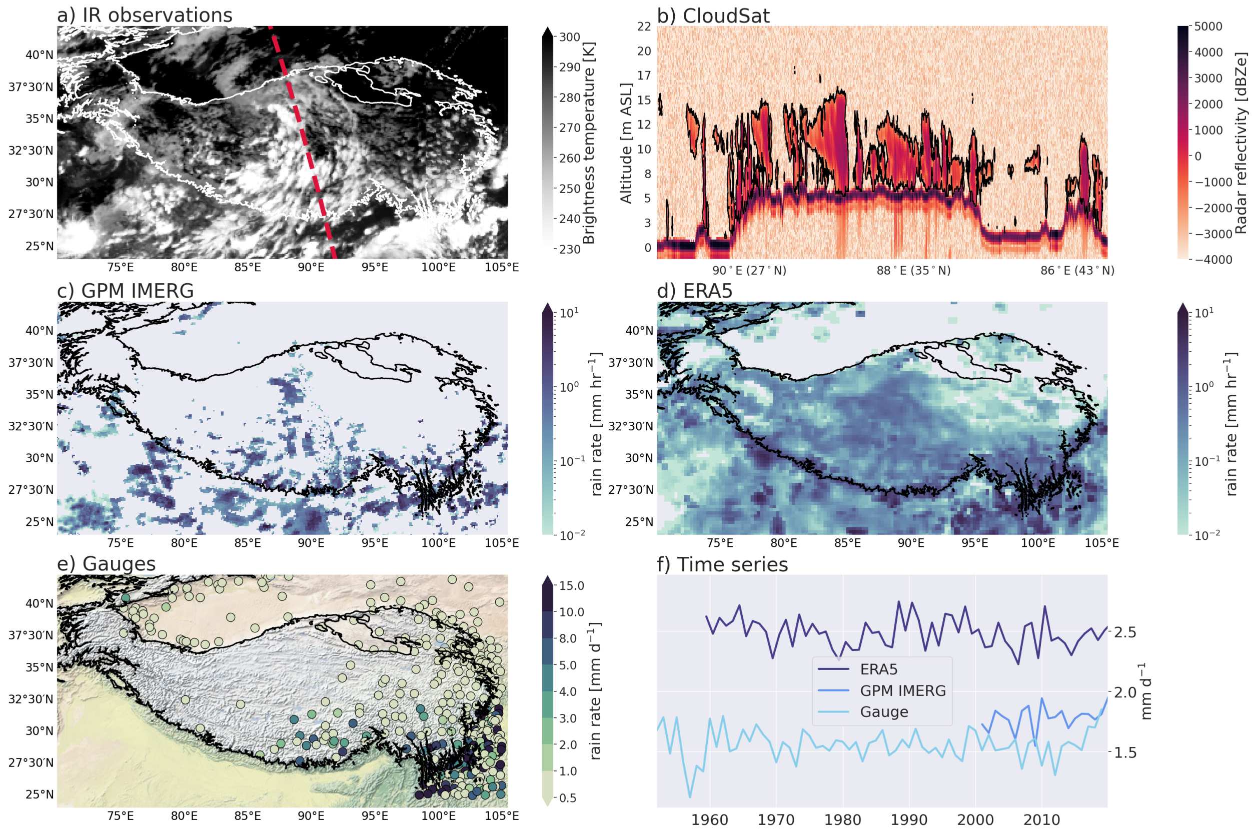

Figure 3.1: Observations of clouds and precipitation over the TP based on different data sources: a) IR brightness temperatures from merged passive satellite observations on July 30^{th}, 2016; 13:00 local time. The red line indicates the trajectory of a CloudSat overpass of which the observations are shown in panel b. b) Convective clouds over the TP during daytime ($\sim$ 13:00 local time) as seen by the radar sensor onboard CloudSat. The panel shows a vertical cross-section of radar reflectivities wherein the black contour marks features that are classified as clouds. Notice that the dark area of high reflectivities just above the surface is due to unwanted echoes from the ground. c) Satellite-retrieved hourly rain rates from GPM IMERG during at the same date and time as in a). d) Hourly rain rates from the global reanalysis ERA5 at the same date and time as in a). e) Accumulated daily precipitation from gauge measurements on the same day as in a). f) Time series with annual mean precipitation averaged over the area shown in a-e for gauge measurements, GPM IMERG, and ERA5.

3.3 Global reanalysis data

Reanalysis data combines observations with numerical models through a technique called data assimilation. These data sets provide a best estimate of the atmospheric state that is both physically consistent (due to the time integration of numerical models solving the underlying physical equations) and constrained by observations.

While reanalyses provide a robust estimate of the large-scale atmospheric circulation and

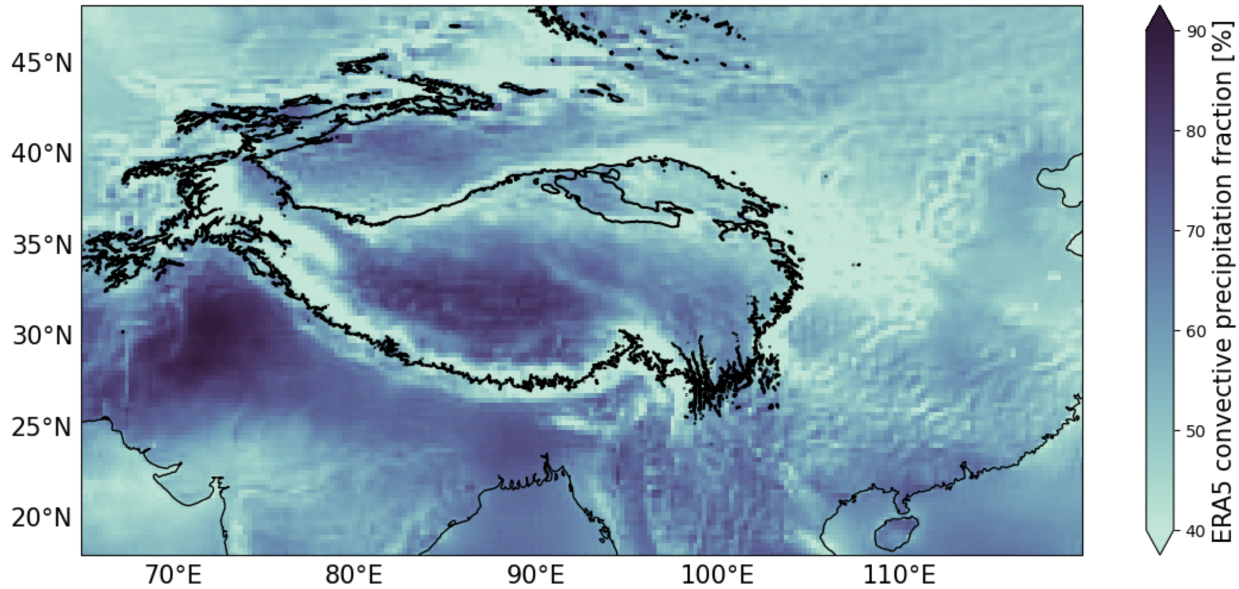

Figure 3.2: Fraction of total annual precipitation that is produced by the convective parameterization scheme in the global reanalysis ERA5 based on monthly averages for the period 1980–2020. This fraction reflects the relevance of convective processes in the region. At the same time, it also reflects the uncertainty of regional precipitation estimates because these estimates are associated with a highly simplified representation of convective processes.

associated water vapor transport, clouds and precipitation are among the most uncertain atmospheric variables in such data sets. Reanalyses have similar uncertainties to conventional global and regional climate models because they rely on the parameterization of convective processes to represent precipitation from convective storms. In other words, they do not explicitly resolve updrafts and convective mass fluxes, but instead, describe the collective effects of convective clouds within a grid cell as a function of the resolved large-scale conditions. Figure 3.2 demonstrates how much of the annual mean precipitation in the ERA5 reanalysis is produced by parameterized sub-grid processes as opposed to precipitation that results from large-scale processes. While precipitation along the Himalayas mainly results from large-scale processes (probably when air masses are pushed against the high orographic barrier; see section 1.3.2), precipitation in the central parts of the TP as well as in the regions south and east of the mountains is largely associated with non-resolved sub-grid processes. This indicates that there is relatively high uncertainty in the precipitation estimates from reanalysis data over the TP. Figures 3.1c-d and f show large differences between precipitation estimates from GPM and ERA5, which reflects these uncertainties.

Additionally, small-scale variations in topography are poorly represented in ERA5 (Fig. 3.3). This shortcoming affects the representation of mesoscale processes associated with topography interactions, e.g. diurnal up- and downslope wind or water vapor transport through a valley. Likewise, other small-scale features of the land surface are poorly represented which can also be relevant for the representation of convection and precipitation when these are the result of land-atmosphere interactions (see section 2.2.3).

3.4 Regional kilometer-scale model simulations

A promising solution to uncertainties caused by the coarse resolution and convective parametrization of global models are regional, non-hydrostatic *km-scale climate model simulations*. These simulations are performed at horizontal resolutions between 1 km and 9 km and in a non-hydrostatic configuration. A *non-hydrostatic* climate model can resolve vertical motions at scales similar to horizontal motions allowing the convective parameterization to be turned off. Often, such simulations are also referred to as *convection-permitting* because they can realistically resolve convective large storms (Prein et al., 2021).

Since the increase of spatial resolution is more computationally feasible for a limited region than for global simulations, it is common to use regional climate models to perform km-scale simulations (Prein et al., 2015). A regional climate model uses information from a global reanalysis or climate model with a coarser spatial resolution to down-scale large-scale climate processes to regional scales. This technique is also called *dynamical downscaling* (Giorgi & Gutowski Jr, 2015) because it uses large-scale climate variables as initial and boundary conditions, but resolves the dynamics of large-scale and mesoscale processes within the model domain. The result of this technique is higher-resolution climate information that is still consistent with the large-scale atmospheric circulation of the driving reanalysis or model. Furthermore, it is possible to constrain the large-scale circulation in the inner model domain not only through the initial and lateral boundary conditions but also through nudging large-scale variables at certain wavelengths to be more similar to those in the driving model. This specific technique is referred to as *spectral nudging* and has been used in **Paper V** and **VI** (more detailed discussion in Chapter 4.2.2).

Due to the steadily increasing computational capabilities, it is now possible to run regional km-scale simulations over multiple decades (Prein et al., 2015). This offers new opportunities to study convective storms in a climate context. In addition to a more realistic representation of convection, a high spatial resolution has also the potential to better represent meteorological variables that are largely affected by mesoscale processes as well as small-scale variations in land surface features and topography. Figure 3.3 exemplifies how variations in topography are represented in high-resolution climate models with different grid spacings compared to reanalysis data. The better representation of the small-scale features in high-resolution models may significantly influence atmospheric water vapor transport over mountain barriers (Lin et al., 2018) and the occurrence and intensity of precipitation (Lucas-Picher et al., 2021).

However, the representation of convective storms in km-scale climate simulations is still a relatively new research field, and there remain challenges in regional climate modeling, particularly with regard to the representation of convective processes. First, regional climate models are strongly dependent on the lateral boundary conditions which are usually provided by a global reanalysis or global climate model. This dependency implies that uncertainties in the driving reanalysis or model transfer to the regional climate model. While global reanalyses provide the best possible estimate of historical climate and large-scale circulation, the uncertainties in data from global climate models are likely much higher.

Second, regional climate models are only indirectly coupled to the global circulation and water and energy cycle (see **Paper V** and **Paper VI**). Although the forcing through the lateral boundary conditions ensures that the model is overall consistent with the global physics, the atmospheric state in the inner model domain can drift away.

Third, convection still depends on multiple parameterization schemes (i.e. microphysics, planetary boundary layer) and several small-scale processes related to convection are not fully resolved. Because most of the parameterization schemes used in high-resolution climate

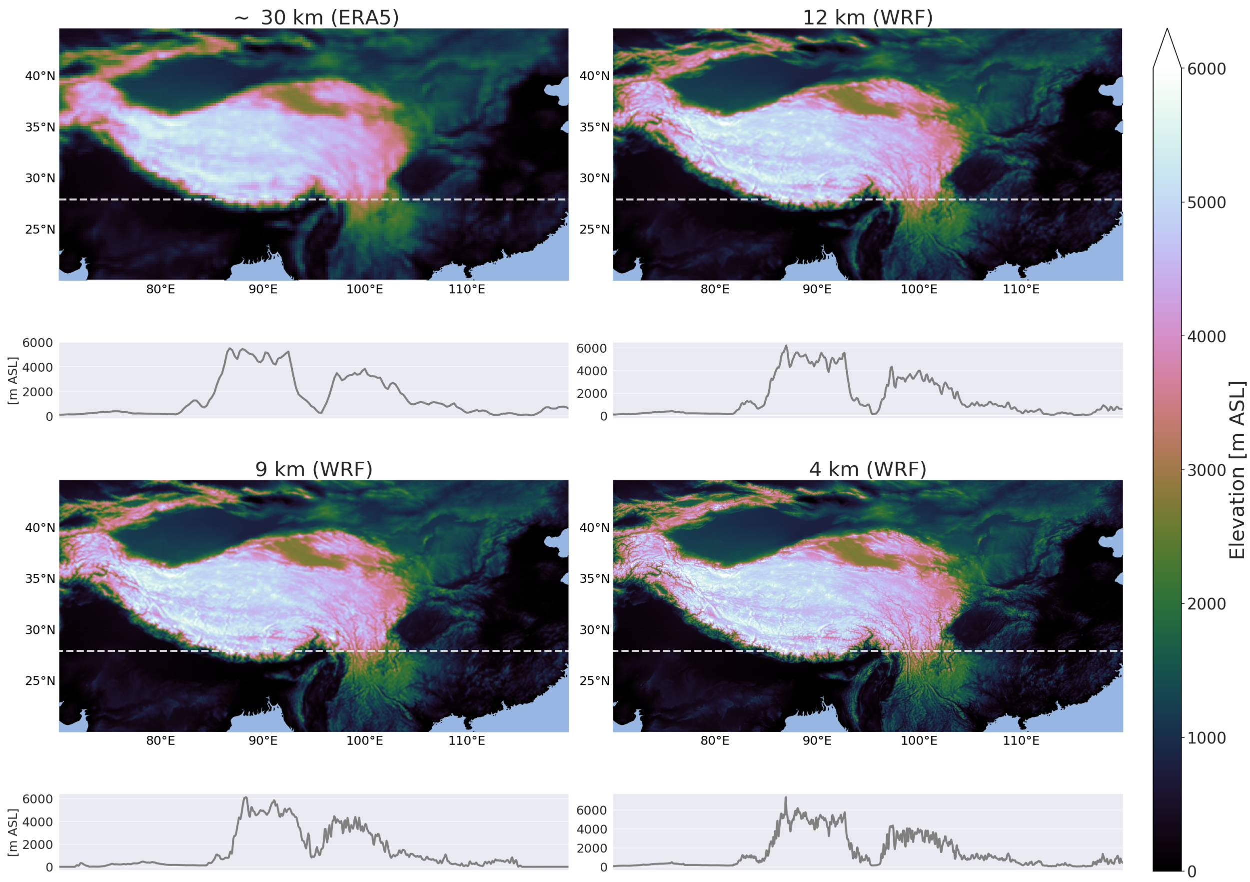

Figure 3.3: Representation of topography in data sets with different spatial resolutions ranging from ~30 km in a global reanalysis (ERA5) to 4 km in a km-scale climate model (WRF). The line plots demonstrate how different the elevation profiles at a given latitude (here: along the gray dashed line at 28°N) compare between the shown data sets.

modeling have been adopted from climate models with coarser spatial resolution, it is still unclear how applicable these are for km-scale models. In addition, it is a topical question which spatial resolution is needed to resolve the most relevant processes to for regional climate change projections.

Finally, there are different techniques for regional climate modeling and many choices have to be made when setting up a model simulation. These choices do not only include choices of parameterization schemes, but also domain size and location, update frequency of lateral boundary conditions as well as horizontal and vertical resolution. All of these choices can affect the model's performance. In **Paper V**, we have used an ensemble of km-scale simulations with multiple models and model configurations to evaluate and discuss their respective impacts on simulations over the TP.

3.5 Observational and model data sets used in this dissertation

Table 3.1 provides an overview of the specific data sets that were used (and partly created) in the scientific papers of this dissertation. These data sets encompass gauge measurements, active and passive satellite observations of clouds and precipitation, global reanalysis data, and km-scale model simulations with grid spacings between 2 km and 9 km.

Table 3.1: Overview of data sets used in the papers of this dissertation

Data source (Parameters)	Name of data product	Resolution	Period	Reference	Paper
Gauge stations (Daily accumulated precipitation)	Chinese Meteorological Agency	-	2000 - 2019	-	III, V
Active satellite measurements (Cloud fraction, Reflectivity)	CloudSat-CALIPSO 2B-GEOPROF-LIDAR	$\sim$ 1 km along track $\sim$ 1 km along track	2006 - 2011	Stephens et al. (2002)	I
Active satellite measurements (Cloud classes)	CloudSat-CALIPSO 2B-CLDCLASS-LIDAR	$\sim$ 1 km along track	2007 - 2010	Stephens et al. (2002)	I
Active satellite measurements (Cloud phase)	CloudSat-CALIPSO 2C-ICE	$\sim$ 1 km along track	2007 - 2010	Stephens et al. (2002)	I
Active-passive merged satellite retrieval (Half-hourly rain rates)	GPM IMERG v06	$\sim$ 11 km	2000 - 2019	Huffman et al. (2019)	II, III, IV, V
Active-passive merged retrieval (3-hourly rain rates)	CMORPH	$\sim$ 11 km	2008, 2011-2016	Joyce et al. (2004)	II, V
Active-passive merged satellite retrieval (Hourly rain rates)	MWSEP	$\sim$ 11 km	2008, 2011 - 2016	Beck et al. (2017)	II, V
Active-passive merged satellite retrieval (Hourly rain rates)	CHIRPS	$\sim$ 11 km	2008, 2011 - 2016	Funk et al. (2015)	V
Passive merged satellite retrieval (Half-hourly brightness temperatures)	NCEP CPC	4 km	2000 - 2019	Janowiak et al. (2017)	IV, V
Global reanalysis (Precipitation, Dynamical variables)	ERA5	$\sim$ 30 km	1979 - 2019	Hersbach et al. (2020)	III, IV, V, VI
Km-scale model (Precipitation, Dynamical variables)	WRF	9 km	1979 - 2019	Ou et al. (2020), Ou et al. (2023)	VI
Regional climate model (Precipitation, Dynamical variables)	WRF	4 km	2019-2020	Prein et al. (2022)	V
Regional (and global) climate models (Precipitation, Dynamical variables)	Multi-model ensemble including WRF	2 km-12 km	July 2008	Prein et al. (2022) Kukulies et al. (2023; Paper V)	V

Chapter 4

PAPER SUMMARIES

This chapter summarizes and connects the seven scientific papers included in the dissertation (see List of Papers, p. iii). Since two central themes are the large-scale atmospheric circulation (see Objective 1) and mesoscale convective systems (see Objective 2) as precipitation controls, the results are organized into these two themes. Note, however, that these themes are also intertwined and simultaneously addressed in some of the papers.

4.1 The role of large-scale atmospheric circulation

4.1.1 Vertical cloud structures in three large-scale circulation regimes

Paper I: Temporal and spatial variations of convection and precipitation over the Tibetan Plateau based on recent satellite observations. Part I: Cloud climatology derived from CloudSat and CALIPSO

Motivation and aim

Convective cloud systems have long been recognized as an important component in the water cycle over the TP (section 1.3.3). Since the effect of clouds on the regional climate and its linkage to precipitation depend on the clouds' macro- and microphysical properties, we examined convection over the TP through the lens of cloud observations. Radar measurements from active satellite sensors provide insights into vertical cloud structures which have the potential to greatly improve the understanding of convection in particular regions (section 3.2). Only a few studies have focused on the vertical distribution of cloud systems over the TP in a climatological context. The goal of this paper was to characterize the seasonal and diurnal variations of different cloud types across the TP. In addition, we aimed to investigate differences between different large-scale regimes.

Method

We have used radar reflectivities and retrieved cloud properties from active satellite sensors to create climatological composites of these for the monsoon and westerly seasons. We then compared the climatological cloud properties between three sub-regions of the TP that are influenced by different large-scale atmospheric circulations and moisture sources using the regional framework proposed by Yao et al. (2013). The regions investigated were the westerly-dominated northern TP, the monsoon-dominated southern TP, and the transition zone that is affected by both large-scale atmospheric systems.

Key results

- **Importance of convection:** The radar reflectivity profiles suggest that convective clouds play an important role over the TP. Figure 4.1 shows the distribution of radar reflectivities at different heights which can be seen as a proxy for cloud density at the corresponding given altitude. A distribution with high reflectivities throughout the atmospheric column indicates thus either more convective cloud types with deep vertical extents or the simultaneous occurrence of shallow and high cirrus clouds. In contrast, higher frequencies centered around lower altitudes are typical for bright bands associated with stratiform cloud layers. Figure 4.1c demonstrates that cloud tops can exceed 15 km ASL and that clouds with extents extending 8 km are relatively common during the monsoon season.
- **Differences between sub-regions with different large-scale circulations:** Figure 4.1 shows that clouds with high vertical extents are most common in the monsoon-dominated south during the monsoon season, whereas the westerly-dominated north exhibits more cloud profiles with stratiform cloud layers. Differences in cloud characteristics between the monsoon-dominated and westerly-dominated sub-regions match with the differences associated with the respective seasons, but we note also that differences between the seasons outweigh the sub-regional (as well as day-night) differences in most examined cloud parameters.

4.1.2 Seasonal and diurnal precipitation characteristics over the TP

Paper II: Temporal and spatial variations of convection, clouds, and precipitation over the Tibetan Plateau from recent satellite observations. Part II: Precipitation climatology derived from global precipitation measurement mission

Motivation and aim

While **Paper I** indicated the presence of convective clouds in the monsoon-dominated southern parts of the TP, the cloud observations only contain limited information on surface precipitation due to unwanted echoes of the radar reflectivity close to the surface (see Fig. 3.1b). In this paper, we complemented the cloud analysis by investigating the spatiotemporal patterns of satellite-retrieved precipitation with the goal to determine sub-regional differences in seasonal and diurnal precipitation characteristics. We also tested if these characteristics are consistent with the cloud observations and the large-scale circulation regime framework used in **Paper I**.

Method

We used precipitation estimates from four different satellite products to compare the seasonal and diurnal variations of precipitation across the TP. We also performed a principal component analysis to detect regional patterns of temporal variations beyond the differences in the total amount of precipitation.

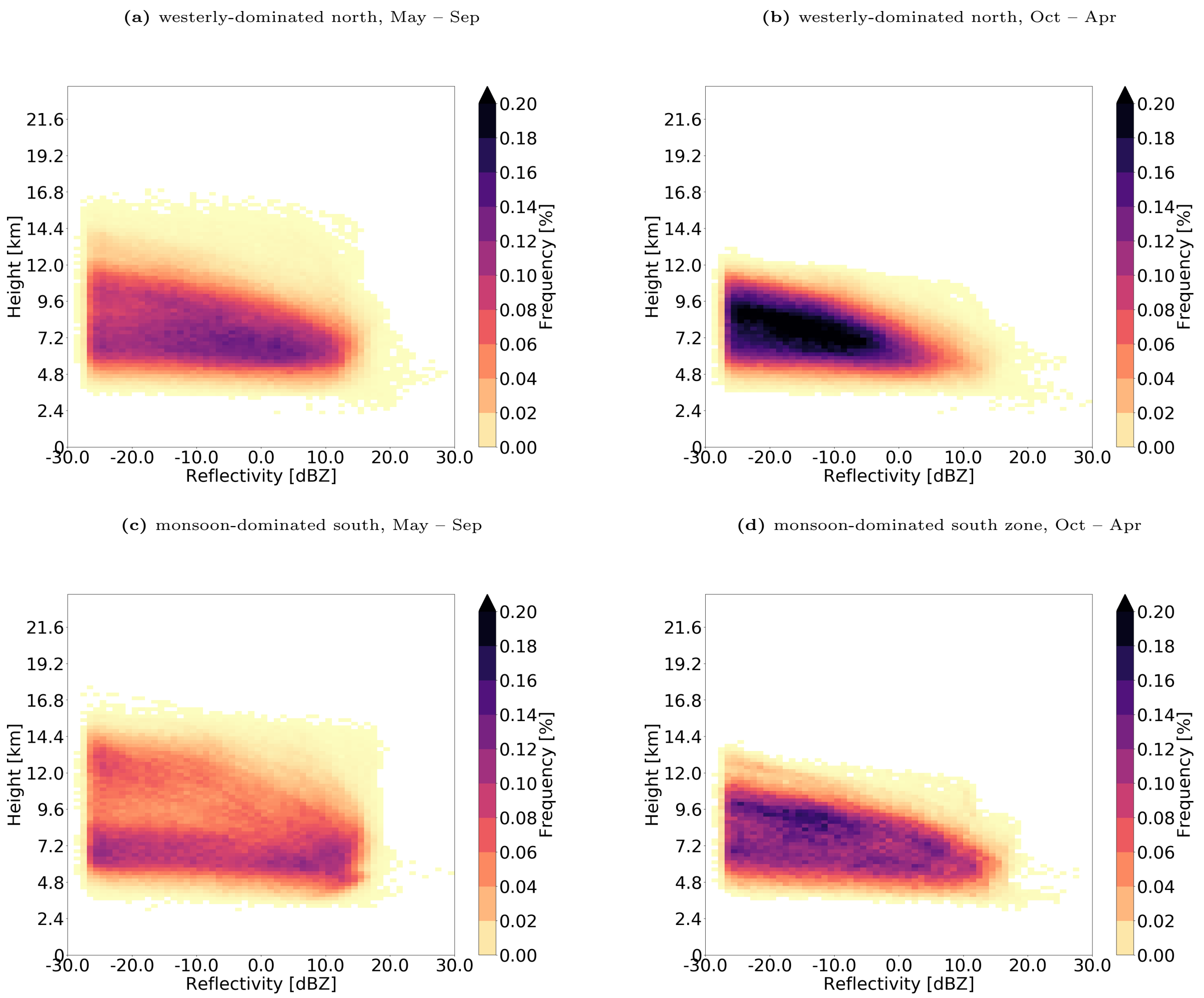

Figure 4.1: Frequencies of radar reflectivity at different altitudes for the westerly-dominated north (a–b) compared to the monsoon-dominated south (c–d) over the TP during monsoon (May-Sep) and westerly seasons (Oct-Apr) based on 2B-GEOPROF (Table 3.1) for 2006 – 2011 (Figure modified from **Paper I**). The height bins [km ASL] of the radar measurements range from 2 km to 17 km with a 0.24 km interval, and the reflectivity bins [dBZ] range from -30 dBZ to 30 dBZ with a 1 dBZ intervals. Higher frequencies concentrated over a narrower range of altitudes indicate stratiform clouds, whereas occurrences of high radar reflectivities distributed over the entire atmospheric column indicate convective clouds.

Key results

- **Sub-regional differences in seasonality:** The differences in seasonal cycles along the west-to-east axis were much more pronounced than along a north-to-south axis, evidencing that the large-scale circulation regime framework used in **Paper I** does not hold for precipitation seasonality. The results of the principal component analysis show a spatial dipole pattern of two distinct seasonalities: The central TP is marked by a strong July peak and more than 70% of the total annual precipitation falls during the monsoon season (May–Sep), whereas the northwestern and southern regions of the plateau exhibit significantly smaller amplitudes in the annual cycle.
- **Sub-regional difference in the diurnal cycle:** The spatial patterns of diurnal precipitation over the TP are more complex and show also a seasonal dependence. During the monsoon season, the diurnal cycle of precipitation over most regions of the TP is distinct from its surroundings. This difference is manifested through a stronger afternoon to early evening peak (17:00 LST time, 11:00 UTC) and a weaker nighttime peak (23:00 LST, 17:00 UTC).
- **Convective precipitation:** Convective precipitation, as classified in the used data products, contributes only between 10 % and 30 % to the total precipitation over the TP during the monsoon months. This is significantly less than previously suggested by climate model simulations and reanalysis data.

4.1.3 Systematic classification of precipitation seasonality

Paper III: Regionalization of Seasonal Precipitation over the Tibetan Plateau and Associated Large-Scale Atmospheric Systems

Motivation and aim

Owing to the importance of the TP for water resources (section 1.3.1), the seasonality of precipitation over the TP has potential implications for the seasonality and magnitude of river runoff. A plateau-scale view on precipitation masks sub-regional differences and one open question is how different large-scale circulation systems affect different regions of the TP. In **Paper II**, we showed that the prevailing precipitation regimes over the TP are more complex than suggested in the large-scale circulation regime framework used in **Paper I**, but it is still unclear which are the dominant large-scale atmospheric systems affecting precipitation and how they influence the inter-annual variability of the prevailing precipitation regimes over the TP. The aim of this study was to answer these two questions by classifying seasonal precipitation regimes in a systematic way and based on multiple data sources.

Method

We have used a self-organizing map algorithm to classify seasonal cycles of 10-day averaged precipitation over the TP in satellite data (GPM IMERG), reanalysis data (ERA5), and gauge measurements. We also performed a composite analysis to relate anomalies in precipitation seasonality to different large-scale atmospheric circulation systems and we quantified how robust different regimes were in terms of inter-annual variations.

Key results

- **Regional precipitation regimes:** Figure 4.2 shows the main result obtained by the classification. Three distinct regional precipitation regimes are 1) a western regime with a winter peak, 2) a southwestern regime with a late summer peak, and 3) an eastern regime with an early summer peak.
- **Inter-annual variations:** The western precipitation regime was the most robust regime with the smallest inter-annual variations, as its extent has not changed much during the past two decades. The extent of the other two regimes tend to shift between the northern and central TP, but are stable in the eastern and southwestern region.
- **Linkage to large-scale atmospheric systems:** The inter-annual precipitation variations in the southwestern and eastern regions were associated with variations in the South Asian high and Indian Summer monsoon, while precipitation variations in the western region were primarily influenced by variations in the westerly jet stream. The main difference between the eastern and southwestern regimes is that the earlier peak of the eastern region was also associated with the anticyclonic circulation over the Western North Pacific and with a stronger South Asian high than the southwestern region.

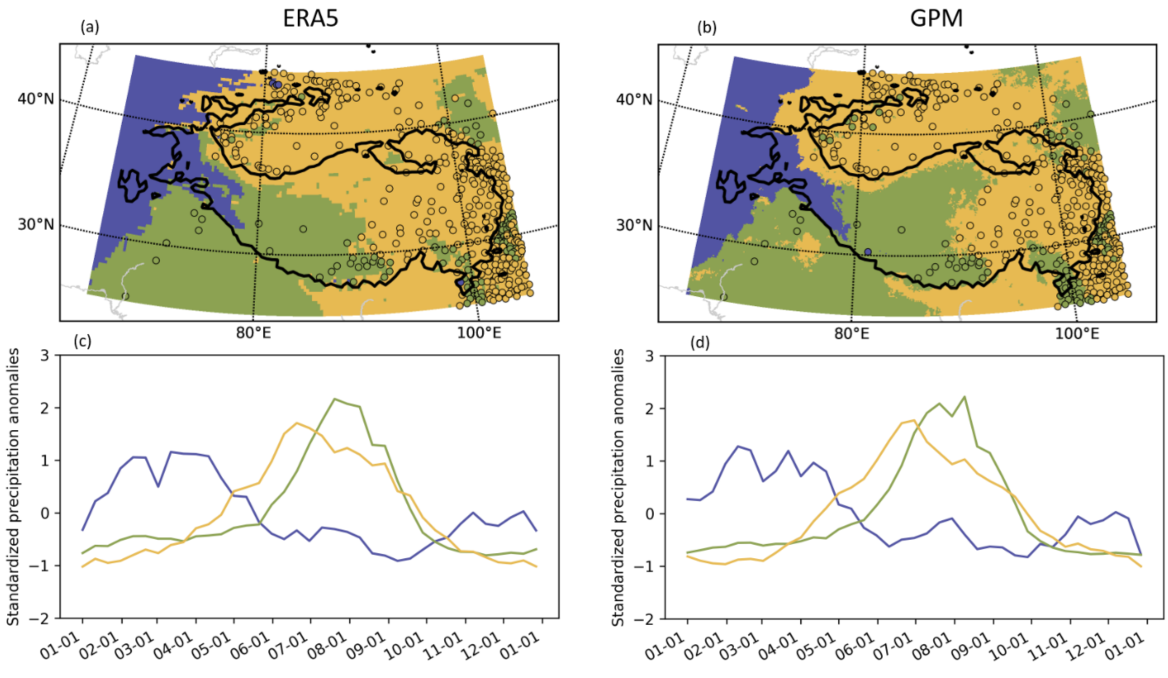

Figure 4.2: Three precipitation seasonality regimes classified based on ERA5, GPM IMERG, and gauge measurements (Figure adopted from **Paper III**). The blue region is primarily associated with the westerly circulation, while the green and yellow regions are both associated with the South Asian High and summer monsoons.

4.2 The role of mesoscale convective systems

4.2.1 Satellite-derived climatology

Paper IV: The Role of Mesoscale Convective Systems in Precipitation in the Tibetan Plateau Region

Motivation and aim

Thus far, we have established a better understanding of how large-scale atmospheric systems are linked to the prevailing cloud and precipitation regimes over the TP, but we have not looked at the downstream regions yet. Mesoscale convective systems (MCSs) have been suggested as an important source of precipitation both over the TP and in its downstream regions, but their characteristics and impact on precipitation are not well understood. From **Paper I**, we know deep clouds occur frequently over the TP, but it remains unclear how large these systems are and if they are primarily associated with MCSs.

Previous studies have mainly used infrared (IR) satellite imagery to identify MCSs over the TP. This can lead to errors because cirrus clouds or other cold features over mountain regions can give signals similar to those of convective systems in warm-climate regions. Therefore, the primary goal of this paper was to clarify the role of MCSs in precipitation. For this, we developed a novel tracking algorithm that makes use of IR brightness temperatures combined with satellite-retrieved precipitation as an additional constraint in the MCS identification. Given the importance of downstream MCS formation (sections 4.2 and 2.2.2), we focused not only on the TP headwaters but also on the surrounding downstream regions.

Method

Using 20 years of half-hourly brightness temperatures from IR satellite imagery combined with satellite precipitation estimates from GPM IMERG, we created an MCS climatology for the TP and its surroundings. We developed a new method to track MCSs over the TP based on the open-source python package *tobac* (Sokolowsky et al., 2023; *Manuscript in preparation*). The resulting tracks were used to derive storm statistics for different sub-regions and to identify large-scale atmospheric circulation systems that were favorable for MCS genesis in the respective regions.

Key results

- **MCS tracking method:** When precipitation and stricter thresholds for brightness temperatures are used as additional constraints in the MCS identification, the results of the tracking show significantly fewer MCSs over the TP compared to when only brightness temperatures are used. This suggests that the role of MCSs over the TP headwaters might have been overestimated in previous studies.
- **MCS-associated precipitation:** The resulting MCS database has been used to derive the contribution of MCSs to the total precipitation. The upper panels in Figure 4.5 show the climatological contribution during the summer months June-August. In some areas, MCSs contribute more than 50 % to the total rainfall, indicating their potential importance for agricultural activities. The regions over land with the highest MCS

contributions are the Indo-Gangetic Plains and the Mekong river basin. In addition, MCSs play an important role in the Sichuan and Yangtze river basins, particularly during the mature phase of the monsoon between June and August. The results of all sub-regions indicate that MCSs that produce the largest amounts of precipitation are characterized by longevity and large extents rather than by high intensities.

- **Linkage to large-scale atmospheric systems:** Anomalies in the location and intensity of the South Asian High and westerly circulation were associated with smaller MCSs that originated over the TP. In addition, strong negative anomalies in 500 hPa geopotential height, widespread positive anomalies in atmospheric instability, and positive anomalies in moisture advection between 20N° and 30 N° were associated with MCSs in the downwind regions.

4.2.2 Kilometer-scale ensemble simulations

Paper V: Kilometer-scale multi-model and multi-physics ensemble simulations of a mesoscale convective system in the lee of the Tibetan Plateau: Implications for climate simulations

Motivation and aim

The climatological importance of MCSs in the eastern and southern downstream regions of the TP was shown based on observations in **Paper IV**. As a next step, we aim to investigate how well climate models can capture MCS characteristics and their impact on precipitation since this is a prerequisite for future climate projections.

Km-scale model simulations provide a useful tool to investigate precipitation processes over and around mountains, where convective organization is influenced by interactions with topography (section 3.4). The aim of this paper was to assess the sensitivity of km-scale simulations of a downstream MCS to different model systems and configurations. In addition, we aimed to identify physical processes that need to be correctly simulated for successfully capturing the downstream MCS formation.

This study was part of an internationally coordinated modeling effort (a so-called CORDEX Flagship Pilot Study) that aims to assess the benefits and limitations of km-scale climate models for simulating the water cycle over the TP.

Method

We have evaluated a km-scale model ensemble of a flood-producing MCS in the east of the TP. This ensemble consisted of 36 simulations using different regional climate models, parameterization schemes, and model setups (e.g. varying domain size and spatial resolution) to analyze how well the MCS and associated processes (e.g. vortex evolution, cloud formation and water vapor transport) were represented. To put this case study in a longer time context, we also evaluated the simulated MCS statistics in a one-year-long simulation performed with the Weather and Research Forecast (WRF) model (Skamarock et al., 2019).

Key results

- **Key processes:** Recall from section 2.2.2 that Tibetan Plateau vortices (TPVs) can influence the downstream weather east of the TP. In this case study, we identified the evolution and transport of a TPV, its interaction with the jet stream, and water vapor advection from the south as key processes for the MCS formation. Figure 4.3 visualizes the eastward propagation of the TPV from the mountains to the lower-elevation areas and the water vapor fluxes into the basin wherein the MCS was observed. The eastward propagation of the TPV is visible as a tilted streak of positive relative vorticity occurring between July $18^t h$ and July 20^{th} in the Hovmöller diagram. The figure compares two WRF simulations to ERA5 and shows that the WRF simulation that is nudged to be closer to the large-scale atmospheric circulation in ERA5 ($\text{WRF}_{nudging}$) captures the vortex transport and the water vapor transport from the south. In contrast, the WRF simulation without nudging does not capture these two processes. This demonstrates the importance of the large-scale circulation for the mesoscale processes involved in this specific MCS case (Fig. 4.3).
- **Model sensitivities:** There were generally large differences between the regional climate models and most simulations struggled to capture the interaction between the vortex and jet stream, resulting in a poor simulation of the location and magnitude of MCS-associated precipitation. Constraining the large-scale flow by spectral nudging and increasing the domain size improved the simulation significantly. This is shown in Figure 4.4 which compares the skill of different models and model configurations in simulating precipitation at different spatial scales.
- **MCS climatology:** Figure 4.5 shows the simulated MCS precipitation in the one-year-long simulation compared to satellite observations. It was found that the identified biases in water vapor transport, vortex evolution, and jet stream in the case simulation did not significantly influence the general statistics of MCS-associated precipitation and associated water vapor transport in the one-year simulation. However, while the seasonal cycle of MCSs and domain-averaged MCS-associated precipitation are well captured, there are biases in MCS occurrences over the TP, south of the Sichuan basin, and south of the Himalayas. These biases in the spatial distribution of MCSs indicate that the model performance may also depend on the mechanism that is relevant for MCS formation in different regions.

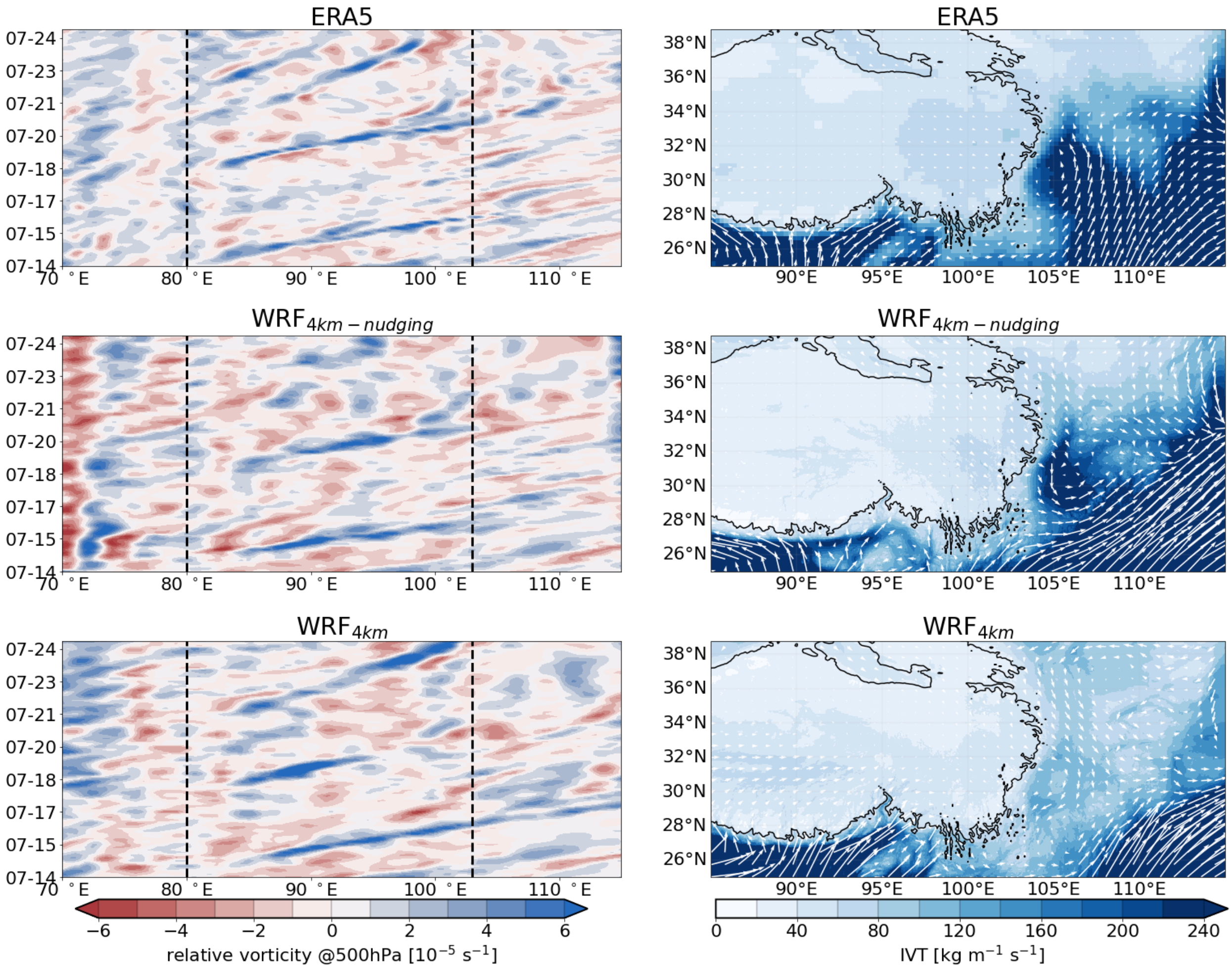

Figure 4.3: Hovmöller (latitude-time) diagrams of relative vorticity [10^{-5} s^{-1}] and mean vertically integrated water vapor transport (IVT) during an MCS event in the Sichuan basin (located in the east of the TP) in July 2008. The panels compare the vortex evolution over the TP (left panels) and the subsequent water vapor transport in the lee of the TP (right panels) between ERA5 and two WRF simulations at 4 km, one of which has used spectral nudging (Figure modified from **Paper V**). The dashed lines in the left panels indicate the western and eastern boundaries of the TP. Notice that the observed time of the MCS event corresponds to the time point when the TPV moves of the plateau in ERA5 (20^{th} July).

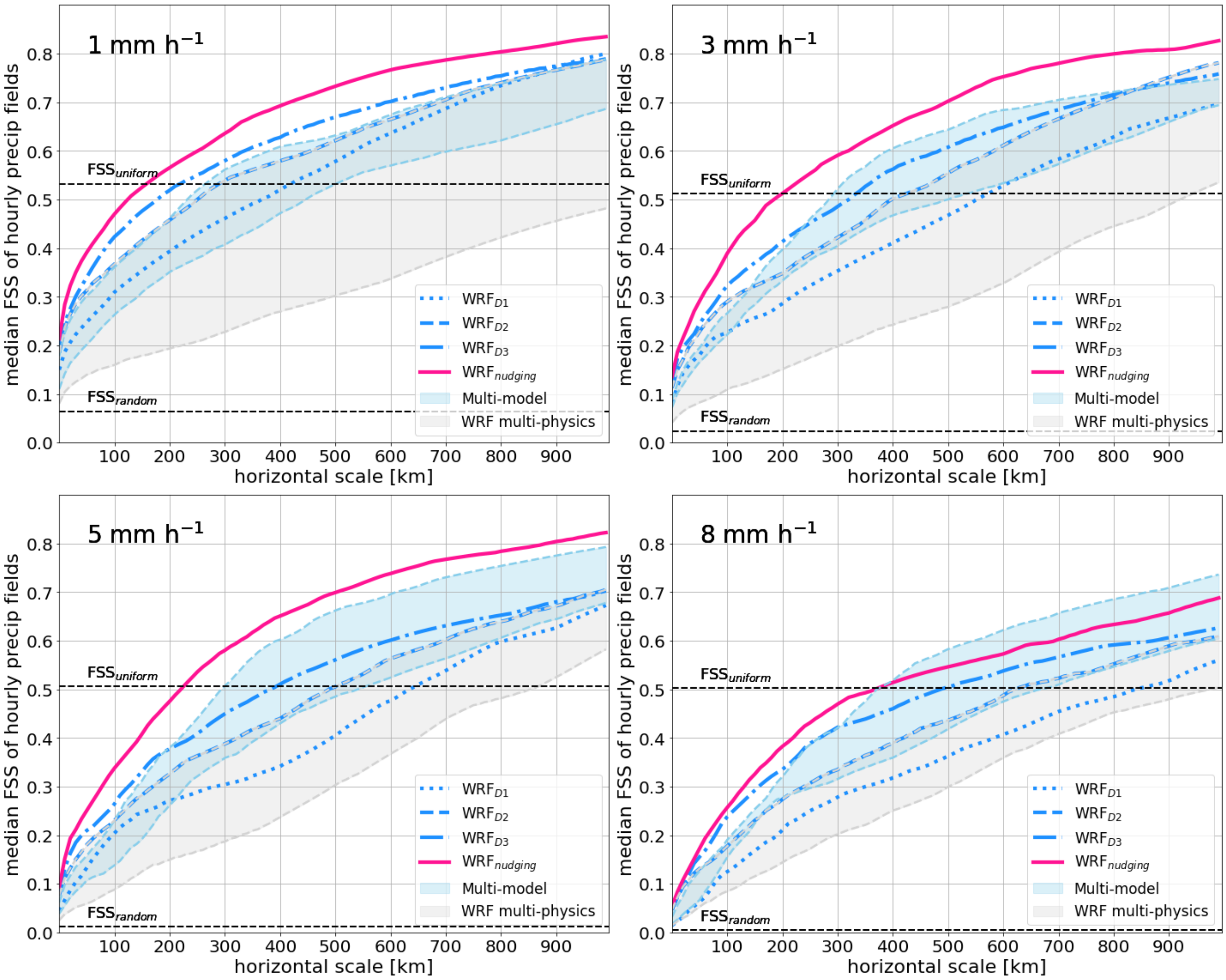

Figure 4.4: Median fractional skill scores (FSSs) of simulated hourly precipitation fields during an MCS event in the lee of the TP (Figure modified from **Paper V**). The FSS is a spatial verification metric that measures the fraction of simulated rain rates above a specified rain rate threshold within a certain neighborhood (horizontal scale) compared to reference observations (here: GPM IMERG; Table 3.1)). The figure shows that WRF simulation using spectral nudging (WRF$_{nudging}$) has the highest skill in the ensemble. Additionally, the simulation was sensitive to the domain size (WRF$_{D1}$ to WRF$_{D3}$, where WRF$_{D1}$ represents the smallest domain) with the higher skills for the larger domain sizes (WRF$_{D2}$ and WRF$_{D3}$). The gray shading indicates the spread of a WRF ensemble with different physics parameterizations and the blue shading indicates the spread of different regional climate models.

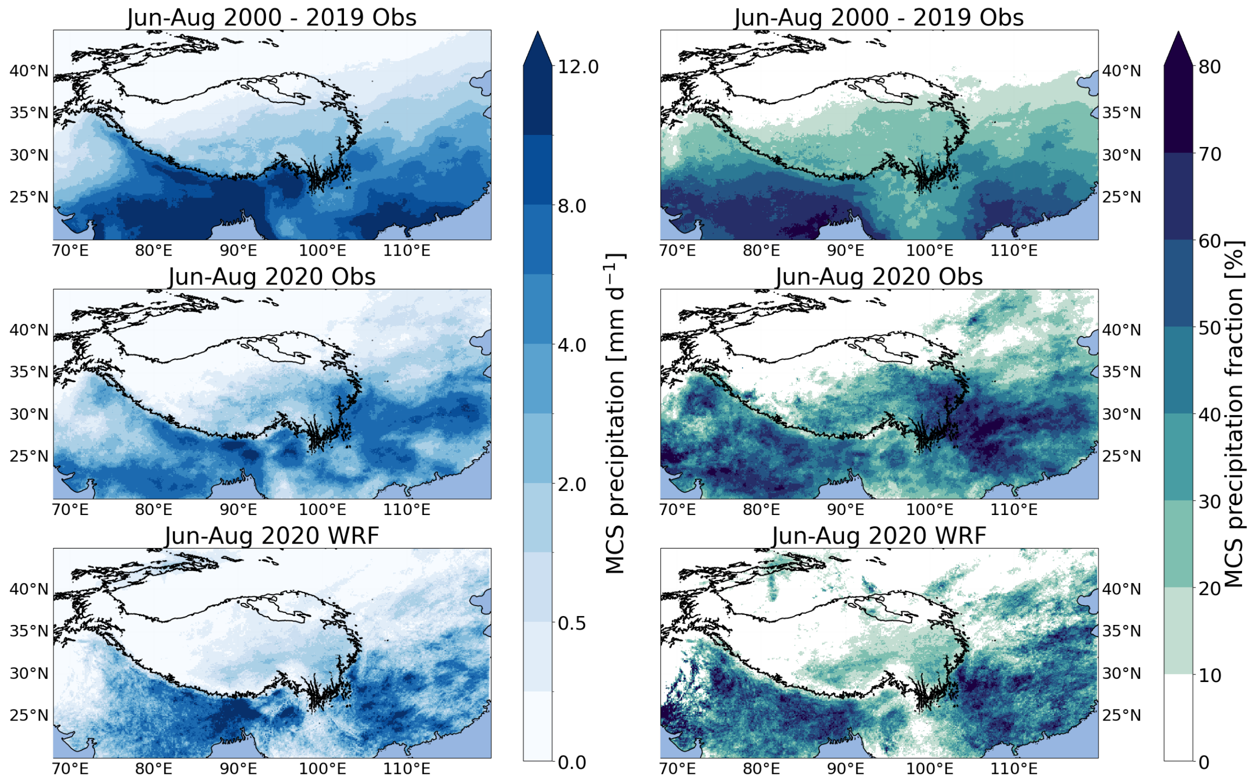

Figure 4.5: MCS-associated precipitation and contribution to total precipitation estimated from satellite observations (Obs) and a km-scale WRF simulation with a horizontal grid spacing of 4 km. The upper panels show the summer climatology for 2000-2019 (obtained from **Paper IV**) and the remaining panels show the summer season for 2020 which was used in the model experiment presented in **Paper V**.

4.2.3 Time scales of summer water vapor transport

Paper VI: Time scales of summer moisture transport downwind of the Tibetan Plateau in reanalysis and dynamically downscaled climate data

Motivation and aim

Paper V left us with the hypothesis that the interaction between the TP and the westerly jet can strengthen cyclonic motion that increases northward water vapor fluxes on the downwind side of the TP. This was motivated by the case study showing that model simulations capturing the TPV transport from the TP into lower-elevation areas showed enhanced water vapor transport from the south. Here, we approached this topic by investigating the importance of turbulent transport in the downwind region east of the TP.

While it is well established that the Asian summer monsoon controls the water vapor transport to the TP region (Fig. 1.2), the role of sub-seasonal time scales of water vapor transport, so-called *eddies*, is poorly understood. This study connects mesoscale with large-scale atmospheric processes by pursuing the following three goals: 1) Determine the relative importance of mean flow and eddies at different time scales, 2) link the time scales of water vapor transport to large-scale atmospheric circulation systems and the atmospheric moisture budget, and 3) investigate the differences in mean flow and eddy water vapor transport between dynamically downscaled and reanalysis data.

Method

We computed the different components of the atmospheric moisture budget and decomposed the horizontal moisture flux convergence (see equation 2.1) and vertically integrated moisture transport into their mean and eddy components at different time scales. To assess regional controls of precipitation in the TP downwind region, the water vapor flux components were calculated for the rectangular latitude-longitude box shown in Figure 4.6. In addition, we calculated the influxes through the southern boundary to this sub-region.

The computed components were correlated with large-scale circulation indices representing variations in the position and intensity of the westerly jet stream as well as different monsoon circulations. Additionally, we linked the water vapor and moisture budget components to MCS frequencies obtained from the data set created in **Paper IV**. The analysis was performed using 40 years of ERA5 reanalysis data and ERA5-driven WRF model output from a non-hydrostatic simulation at 9 km (WRF_{9km}).

Key results

- **Relative importance of mean flow and eddies for water vapor transport:** The mean flow stands for 80 % and the eddy transport 20 % of the total summer water vapor transport. Turbulences at time scales ≥ 3 days contribute ∼50 % of the total eddy transport, whereas shorter time scales stand for the remaining 50 %. Daily to 3-daily eddies show the largest contributions among the studied time scales. Figure 4.6 demonstrates that the downwind region of the TP is a key region for northward sub-daily and daily eddy transport and that the mean flow mainly controls the moisture influx from the south.
- **The role of water vapor transport in precipitation and MCSs:** Summer mean precipitation and MCS occurrences in the downwind region are positively correlated to the mean-flow moisture flux convergence and moisture fluxes from the south. In contrast, MCS occurrences are negatively correlated with eddy convergence and influx through the southern boundary. This means that a higher MCS activity in the downwind region is associated with a higher eddy divergence (i.e. water vapor transported out of the region). As opposed to our hypothesis, the eddy inflow from the south is not significantly correlated with MCS frequencies, suggesting that the mean flow plays a bigger role in total MCS occurrences.
- **Correlations to large-scale circulation indices:** The position of the westerly jet over the TP and the South Asian summer monsoon are negatively correlated with daily and sub-daily eddy divergence and eddy moisture inflow through the southern boundary. This implies an enhanced southerly eddy inflow, but a weaker eddy divergence when the jet is located closer to the equator and when the South Asian monsoon circulation is less strong. In addition, the mean flow convergence in the downwind of the TP is positively correlated with the Western North Pacific monsoon circulation that was also found to play a role in precipitation over the TP (**Paper III**).
- **Differences between ERA5 and WRF:** ERA5 and WRF_{9km} show similar spatial patterns (Fig. 4.6) and the same relative contributions of time scales of moisture transport. However, the moisture transport components in WRF_{9km} shows weaker correlations to the large-scale circulation indices and to precipitation.

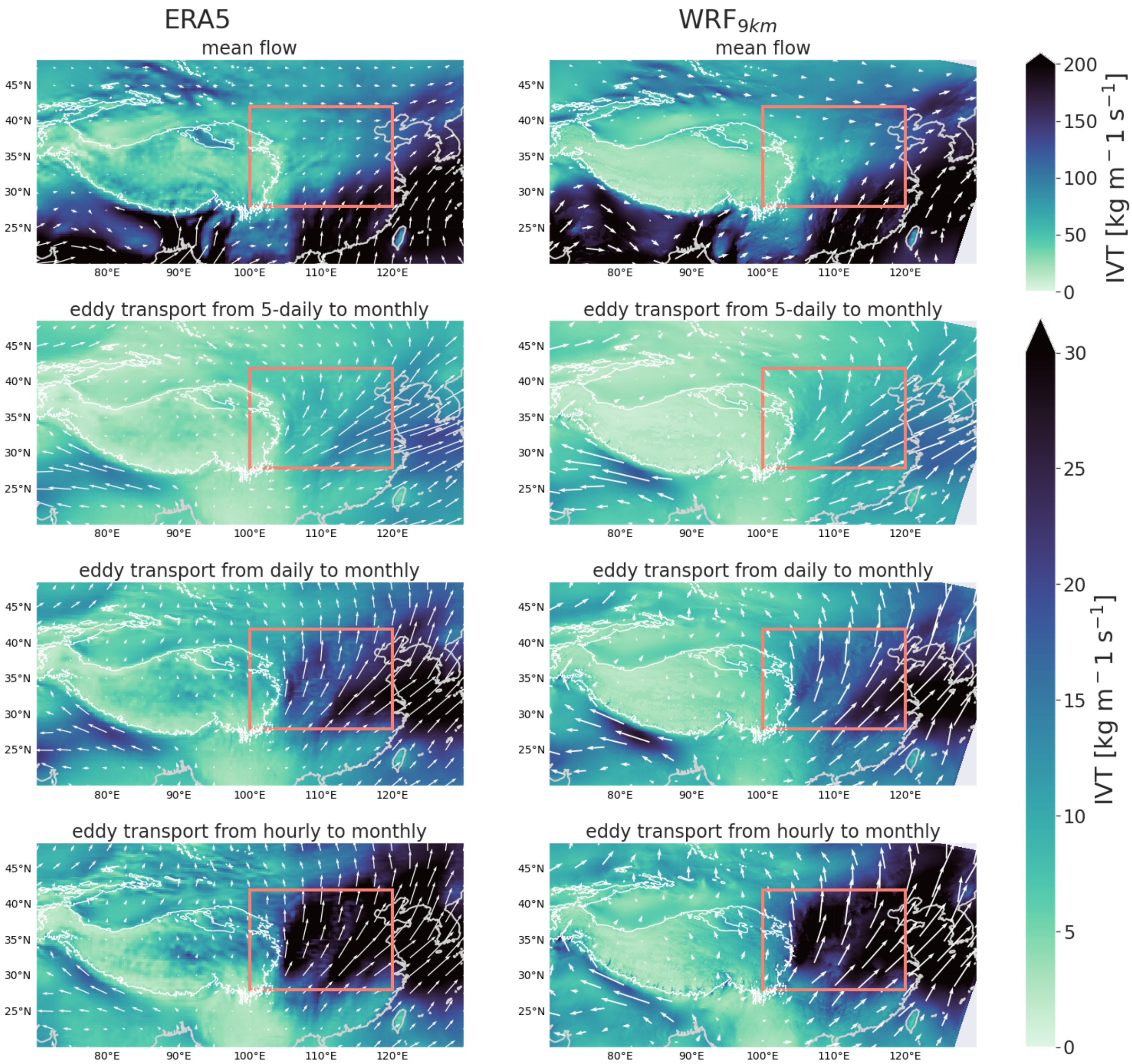

Figure 4.6: Climatology of mean flow and eddy transport computed from different time scales in ERA5 and a 9 km-WRF simulation Figure modified from **Paper VI**). The figure shows that the downwind side of the TP is a key region for eddy transport at daily and sub-daily time scales during summer. The orange box shows the region of interest for which the water vapor fluxes have been calculated. Note that different color bars are used for mean flow and eddy transport because the mean flow contributes significantly more to the total water vapor transport than the eddy transport.

4.2.4 Characteristics, mechanisms, and impact on precipitation

Paper VII: Mesoscale convective systems in the Third Pole region: Characteristics, Mechanisms and Impact on Precipitation.

Motivation and aim

Two major outcomes of this dissertation were the MCS dataset created in **Paper IV** and the model evaluation presented in **Paper V**. In particular, we have shown the importance of downstream MCSs in both seasonal and extreme precipitation and we have proposed processes that could be major factors in MCS formation east of the TP (i.e. jet dynamics, TPV formation, and southerly water vapor transport). In addition, we have shown and discussed potential issues related to MCS identification in IR satellite imagery (**Paper IV**) and the representation of MCSs in km-scale model simulations (**Paper V**).

These results were contextualized and compared to other observational and model studies of MCSs in the TP region in this review paper. The goal was to present critical knowledge gaps that need to be addressed as we proceed with regional climate change assessments in the TP region. More specifically, we reviewed the different methods used for MCS identification, present-climate characteristics of MCSs derived from multiple satellite-based climatologies, processes that favor MCS genesis, and the impact of MCSs on seasonal and extreme precipitation over the TP headwaters compared to its downstream regions.

Key results

- **Comparison of MCS tracking methods:** Due to the usage of different identification and tracking methods, MCS frequencies and contribution to total precipitation varies significantly between different studies. The absence of a common standard to identify and track MCSs is a challenge in the results from the current literature that is not only limited to the TP region and makes it difficult to compare different studies.

  In the TP region, there might have been an overemphasis of MCSs over the headwaters and drier regions due to tracking methods that use only brightness temperatures as a proxy for convection. This is because commonly used criteria to identify MCSs over warm-climate regions result in an overestimation of MCSs in high-altitude regions. There is evidence that convection occurs in an isolated and scattered manner rather than in the form of well-organized MCSs over the TP. However, the spatial scales of different convective modes over the TP and their role on downstream MCS formation remain to be addressed in future research.

- **Identified knowledge gaps:** Thus far, MCSs in the TP region have not been studied under different future climate scenarios. Three identified knowledge gaps that will be crucial to address in future climate projections are 1) the feedback effects of MCSs to other components of the TP climate system, 2) the impact of the changing climate on MCS frequency and intensity, and 3) the assessment of potential flood and drought risks at the basin-scale associated with these changes.

- **Km-scale model simulations:** Multiple high-resolution data sets exist over the TP, some of which are performed at horizontal spatial resolutions below 10 km. We provide suggestions on how these data sets can be used to systematically evaluate the representation of MCSs in historical simulations, in order to provide a basis for the development and interpretation of future simulations.

Chapter 5

CONCLUSIONS

Turning back to the three main objectives listed in section 1.4, the main conclusions from this dissertation can be summarized as follows:

Large-scale atmospheric processes associated with precipitation

- The westerly jet was identified as a major large-scale atmospheric system affecting precipitation regimes in the northwestern TP (**Paper VI**), the formation of MCS over and in close vicinity to the TP (**Paper V**, **Paper VII**), the transport of a TPV that lead to subsequent downstream MCS formation (**Paper VI**), and eddy water vapor transport in the downwind region of the TP (**Paper VI**).
- The South Asian High, the South Asian summer monsoon, the East Asian summer monsoon, and westerly jet were identified as controls for seasonality and inter-annual variability of precipitation in three different regional regimes over the TP (**Paper III**). While the large-scale circulation regime framework suggested by Yao et al., 2013 matches with the north-south disparities of cloud properties over the TP (**Paper I**), it cannot explain precipitation seasonality in different sub-regions of the TP (**Paper II**, **Paper III**).
- Enhanced mean-flow water vapor influxes from the south were identified as a control for mean precipitation and MCS occurrences in the downwind region of the TP (**Paper VI**). This is consistent with the results from **Paper IV** showing positive anomalies in water vapor transport over land when MCSs occur east of the TP. In addition, anomalous water vapor influxes from the south were associated with an off-moving TPV and subsequent flood-producing MCS case at the eastern edge of the TP (**Paper V**). However, there was no significant correlation between eddy water vapor influxes from the south and MCS occurrences in a longer time context (**Paper VI**).
- In general, the results of the different studies point to interactions between the large-scale atmospheric systems because the aspects of precipitation and convection were in most cases not associated with one particular system.

The impact of MCSs on precipitation

- Large MCSs are more frequent in the downstream regions than over the TP, where convection occurs at smaller spatial scales (**Paper IV**). In addition, MCSs produce significantly higher amounts of total precipitation in the downstream regions.

- In some of the downstream regions, MCSs contribute with more than 50 % to the total summer precipitation, showing that MCSs play a vital role in the water cycle in those regions (**Paper IV**; Fig. 4.5).

The ability of km-scale models to simulate precipitation and related processes

- The evaluation of a specific flood-producing MCS case demonstrated that the performance of km-scale simulations in simulating MCSs can be strongly dependent on the underlying regional climate model and model configuration. The domain size and the degree of large-scale constraint (e.g. through spectral nudging or a high update frequency of lateral boundary conditions) were identified as the main factors influencing the simulation over the TP (**Paper V**). This has to be considered in future climate simulations.
- The general patterns of summer precipitation, water vapor transport from the south as well as the domain-averaged MCS frequencies and MCS contributions to precipitation were well captured in a one-year-long WRF simulation compared to satellite observations. However, biases in MCS occurrences over the TP, in the lower Sichuan basin and south of the Himalayas indicate that the model performance differs in regions wherein different MCS mechanisms dominate. Since such differences in model performance are likely to affect the projected climate change response of MCSs, this needs to be considered in the evaluation of future climate simulations (**Paper V**).
- Truthful representation of large-scale dynamics within the high-resolution model were found to be necessary for realistic modeling of meso-scale phenomena. Therefore, regional climate modeling projects must find a balance between keeping the high-resolution simulation ufficiently close to the forcing simulation while not eradicating the potential benefits of high spatial resolution. For example, the simulated westerly jet dynamics over the TP were crucial to correctly simulate a flood-producing MCS case at its downwind side (**Paper V**).

Chapter 6

DISCUSSION AND PROSPECTS FOR FUTURE RESEARCH

6.1 The added value of km-scale simulations

Although km-scale climate model simulations have generally been shown to improve simulations of short-term and heavy precipitation, orographic precipitation, and the onset of summer convection (Lucas-Picher et al., 2021; Prein et al., 2015), their *added value*, i.e. their improvement with regard to coarser resolution simulations, is often dependent on the study region and model configuration (Lucas-Picher et al., 2021). For the TP region, the *added value* of km-scale climate model simulations remains to be confirmed, even though some studies indicate that the diurnal cycle and orographic precipitation are improved in these simulations (Li et al., 2021; Zhou et al., 2021).

While we have not specifically addressed the question of *added value* in our model evaluation, the results from **Paper V** highlight that the model performance of a particular MCS case was strongly dependent on the regional climate model, the model configuration (i.e. domain size) and the applied downscaling technique (i.e. the use of spectral nudging). Of course, this case does not necessarily reflect the ability of the models to correctly model MCS statistics over longer time scales. However, it demonstrates that specific MCS ingredients (in this case: vortex transport and water vapor fluxes) are not well captured in certain configurations. While the general MCS statistics in a single one-year simulation were reasonably well captured compared to satellite observations, a critical next step will be to quantify the uncertainty in this simulation based on additional one-year-long simulations performed with other regional climate models and model setups.

Further, the results of the one-year-long MCS climatology showed biases in MCS occurrences in particular regions that are likely affected by different mechanisms for MCS formation (**Paper V**). This suggests that the *added value* of km-scale models in representing MCSs may also depend on the processes involved for MCS formation. In other words, some processes leading to MCS formation might be better captured by a particular simulation than others. To give an example from another region: Km-scale climate model simulations over North America successfully captured MCSs that were forced by the large-scale circulation, whereas they failed to represent MCSs that were forced by local mesoscale circulations and land-atmosphere interactions (Barlage et al., 2021; Prein et al., 2020). The evaluation of model processes rather than just precipitation as their outcome, is, therefore, needed to interpret and improve high-resolution climate models. Object-based analyses such as the MCS tracking in **Paper V** complement the evaluation of climate models based on general precipitation metrics (e.g. accumulated precipitation), because these do not reflect differences in the simulated processes leading to precipitation formation.

Several results of this dissertation highlight the importance of the large-scale atmospheric circulation for regional precipitation: 1) **Paper III** demonstrated that the inter-annual variability in seasonal precipitation regimes correlated with different large-scale systems such as the South Asian High, westerlies, and South and East Asian summer monsoons. 2) **Paper IV** demonstrated that MCSs in the vicinity of the TP are associated with the position and intensity of the South Asian High and the westerly jet stream. 3) **Paper V** showed that the simulation of a lee side MCS was significantly improved when the large-scale circulation was constrained by spectral nudging. 4) **Paper VI** showed that variations in mean flow and eddy water vapor transport correlate with variations in the Western North Pacific Monsoon and the position of the westerly jet over the TP. All of these results collectively suggest that a realistic representation of the large-scale atmospheric circulation is key to correctly simulating the regional precipitation patterns over and around the TP. In theory, a high-resolution regional climate model should contain the same or similar large-scale features as its driving reanalysis or model (Denis et al., 2002). However, the model can also develop mesoscale processes that feed back to the large-scale circulation in a way that it drifts away from its forcing data. An essential question in km-scale modeling is thus how we can assure a realistic simulation of large-scale atmospheric features while not eradicating potential benefits of the high-resolution simulations.

Global km-scale models have the advantage over regional models in that they have a physically more consistent large-scale circulation. However, global km-scale simulations are currently only performed over limited time periods due to the considerably higher computational costs than regional simulations (Kendon et al., 2017). In addition, reanalysis-driven regional km-scale models are more consistent with the observed state of the atmosphere, as they are forced by a large-scale circulation that has been corrected for observations (section 3.3). Given the respective advantages of regional and global km-scale simulations, a scientific question that should be addressed in future research is how the large-scale and mesoscale structures of precipitation and convection compare in these two types of simulations.

An open question that has still not been fully resolved is whether an improved representation of precipitation in km-scale models can really be attributed to the better representation of deep convection. For the TP region, it will be particularly interesting to quantify to which extent such improvements can be related to a better representation of convection as opposed to a better representation of the topography. Since improvements in precipitation could also be the result of parameter tuning, it is useful to study model biases based on simulations with various model configurations.

Ensemble-based simulations that include different models, configurations, and parameterization schemes (see **Paper V**) allow for a systematic evaluation of km-scale simulations. They help to get a more holistic understanding of the remaining challenges in regional climate modeling and to define the *added value* of km-scale climate models based on multiple aspects and verifications. **Paper V** showed, for instance, that the use of spectral nudging in a one-year simulation reduced some of the regional biases in MCS occurrences, while the biases in MCS-associated precipitation were generally higher compared to the same model realization without nudging. This illustrates that it is not always trivial to determine if a simulation is improved, and an important question that we need to address is whether the detected improvement in a particular variable comes at the expense of another.

6.2 Convection-Permitting Third Pole

The high computational costs of the km-scale simulations and the large data volumes of the model output (Prein, Rasmussen, & Stephens, 2017) limit the capabilities of individual research groups to perform longer-term simulations using multiple setups. Therefore, it is useful to coordinate modeling projects between research communities. Lucas-Picher et al. (2021) highlight *CORDEX Flagship Pilot studies* as a successful example for bringing together smaller research communities on critical scientific questions in targeted regions. The project *Convection-Permitting Third Pole (CPTP)* presented in **Paper V** is one of the currently ongoing Flagship pilot studies with the goal to assess the benefits and limitations of km-scale models to simulate the TP water cycle. The evaluation of the case study and one-year simulation presented in **Paper V** was one of the first steps to find an optimal setup for a long-term climate projection for the TP. The planned future projection will provide new insights into how atmospheric processes discussed in this dissertation (e.g. mountain convection, lee side MCS formation, and seasonal to sub-seasonal water vapor transport) will change in a warmer climate. Hence, the appended scientific papers of this dissertation may guide the research priority-setting for the analysis of future simulations over the TP.

A particular focus will be on future changes in the frequency, intensity, and spatial distribution of MCSs in the TP region. Shifts in the large-scale atmospheric circulation are particularly important to consider because MCSs were shown to be linked to large-scale water vapor transport (**Paper IV**, **Paper VI**), the westerly jet and South Asian high (**Paper V**), and other large-scale factors discussed in the review in **Paper VII**. In addition to these dynamical factors, thermodynamic factors such as atmospheric instability will also change in a warmer climate (Chen et al., 2020). **Paper IV** indicated that MCSs over and in the lee of the TP are associated with widespread positive anomalies in atmospheric instability. While these were most likely linked to the large-scale atmospheric circulation, global warming will also affect the mean conditions of atmospheric instability. In the lee of the Rocky Mountains, it has, for instance, been shown that both atmospheric instability and conditions that inhibit convection (section 2.2.2) increase even in the absence of large-scale and mesoscale variations (Rasmussen et al., 2020). These changes cause a future decrease in moderate convection (due to the convective inhibition) and an increase in severe convection due to the higher levels of energy that can accumulate and be released once convection is initiated (Rasmussen et al., 2020).

6.3 Bridging the gap between observation and model communities

Given that km-scale simulations that cover multiple decades have emerged relatively recently, their potential and limitations have not been fully explored yet. Continuous and consistent observations are essential for the development of model parameterizations and the validation of model output. We noticed, for instance, that the spread among different observational data sets over the TP was a considerable source of uncertainty in the model evaluation of the CPTP project Prein et al. (2022). Closer cooperation between observational and model communities is thus a crucial step to ensure that useful observations are produced and used for the purpose of model evaluation.

The full potential of existing satellite observations has likely not yet been used. There is a number of data sets beyond the commonly used gridded data products like GPM IMERG (section 3.2) that could be used to assess the representation of convective processes in climate models from different angles. In particular, active satellite observations (see section 3.2, **Paper I**) could be used to explore how well the vertical structure of different convective storm types is captured. Cloud observations in general seem to remain relatively unused for the purpose of evaluating km-scale climate models, even though they could provide a useful complement to observations of surface precipitation.

6.4 Actionable science?

High-resolution climate models do not only enhance our understanding of physical processes, they are also an important tool for climate adaptation and real-life applications such as flood and water management (e.g. Dale, 2021; Orr et al., 2021). The ultimate purpose of km-scale modeling is thus to create "digital twins" of the Earth system that represent regional-scale climate features as realistically as possible, in order to produce information that can be used by policy- and decision-makers. The act of creating climate information for specific end-users and societal applications is often referred to as *climate service* or *actionable science* (Chen et al., 2021; Shukla et al., 2021). The key idea behind *actionable science* is to prepare end-users for changes in weather and climate and to assist their decision-making based on scientific knowledge.

This dissertation addresses scientific topics such as model uncertainty and multi-scale interactions of atmospheric processes. While the outcome is admittedly not of direct relevance for decision-makers, some of the key findings can be regarded as a prerequisite to design and produce *actionable science* in mountain regions. For example, **Paper IV-VI** discuss the role of MCSs and related processes in different sub-regions, which will help define research priorities for future regional climate change assessments in the TP region. In addition, the process-based model evaluation (see **Paper V** and **VI**) provides a basis for addressing remaining uncertainties in modeling precipitation over and in the vicinity of complex terrain.

In **Paper VII**, we identified the impact of MCS-induced rainfall on river runoff and flooding in the TP region as a major knowledge gap. Hence, an important future research path towards *actionable science* is the assessment of basin-scale flood and drought risks associated with shifts in future storm populations. For this, it will be necessary to investigate the impact of MCSs on flash floods, as has been done in other regions (Dougherty & Rasmussen, 2019; Hu et al., 2021, e.g.). In **Paper IV**, we showed that a single flood-producing MCS contributed to a quarter of the annual rainfall in a river basin at the eastern edge of the TP. However, the total amount of MCS-associated precipitation during this particular event was considerably smaller than in most of the MCS cases occurring regularly south of the Himalayas (**Paper IV**). This demonstrates that other hydrological factors than the total amount of precipitation over time influence whether or not an MCS represents a flood risk.

BIBLIOGRAPHY

Allen, M. R., & Ingram, W. J. (2002). Constraints on future changes in climate and the hydrologic cycle. *Nature*, *419*(6903), 224–232.

Barlage, M., Chen, F., Rasmussen, R., Zhang, Z., & Miguez-Macho, G. (2021). The importance of scale-dependent groundwater processes in land-atmosphere interactions over the central united states. *Geophysical Research Letters*, *48*(5), e2020GL092171.

Barry, R. G. (1992). *Mountain weather and climate*. Psychology Press.

Barton, E., Taylor, C., Klein, C., Harris, P., & Meng, X. (2021). Observed soil moisture impact on strong convection over mountainous tibetan plateau. *Journal of Hydrometeorology*, *22*(3), 561–572.

Beck, H. E., Van Dijk, A. I., Levizzani, V., Schellekens, J., Miralles, D. G., Martens, B., & De Roo, A. (2017). Mswep: 3-hourly 0.25 global gridded precipitation (1979–2015) by merging gauge, satellite, and reanalysis data. *Hydrology and Earth System Sciences*, *21*(1), 589–615.

Beck, H. E., Wood, E. F., McVicar, T. R., Zambrano-Bigiarini, M., Alvarez-Garreton, C., Baez-Villanueva, O. M., Sheffield, J., & Karger, D. N. (2020). Bias correction of global high-resolution precipitation climatologies using streamflow observations from 9372 catchments. *Journal of Climate*, *33*(4), 1299–1315.

Berg, P., Moseley, C., & Haerter, J. O. (2013). Strong increase in convective precipitation in response to higher temperatures. *Nature Geoscience*, *6*(3), 181–185.

Bessho, K., Date, K., Hayashi, M., Ikeda, A., Imai, T., Inoue, H., Kumagai, Y., Miyakawa, T., Murata, H., Ohno, T., et al. (2016). An introduction to himawari-8/9—japan's new-generation geostationary meteorological satellites. *Journal of the Meteorological Society of Japan. Ser. II*, *94*(2), 151–183.

Bibi, S., Wang, L., Li, X., Zhou, J., Chen, D., & Yao, T. (2018). Climatic and associated cryospheric, biospheric, and hydrological changes on the tibetan plateau: A review. *International Journal of Climatology*, *38*, e1–e17.

Carlson, T., Benjamin, S., Forbes, G., & Li, Y. (1983). Elevated mixed layers in the regional severe storm environment: Conceptual model and case studies. *Monthly weather review*, *111*(7), 1453–1474.

Cheeks, S. M., Fueglistaler, S., & Garner, S. T. (2020). A satellite-based climatology of central and southeastern us mesoscale convective systems. *Monthly Weather Review*, *148*(6), 2607–2621.

Chen, D., Rojas, M., Samset, B., Cobb, K., Diongue, A., Niang, A., Edwards, P., Emori, S., Faria, S., Hawkins, E., et al. (2021). Framing, context, and methods. in climate change 2021: The physical science basis. *Contribution of Working Group I to the Sixth Assessment Report of the Intergovernmental Panel on Climate Change*, 215.

Chen, J., Dai, A., Zhang, Y., & Rasmussen, K. L. (2020). Changes in convective available potential energy and convective inhibition under global warming. *Journal of Climate*, *33*(6), 2025–2050.

Curio, J., Schiemannm, R., Hodges, K. I., & Turner, A. G. (2019). Climatology of tibetan plateau vortices in reanalysis data and a high-resolution global climate model. *Journal of Climate*, *32*(6), 1933–1950.

Dale, M. (2021). Managing the effects of extreme sub-daily rainfall and flash floods—a practitioner's perspective. *Philosophical Transactions of the Royal Society A*, *379*(2195), 20190550.

Denis, B., Laprise, R., Caya, D., & Côté, J. (2002). Downscaling ability of one-way nested regional climate models: The big-brother experiment. *Climate Dynamics*, *18*(8), 627–646.

Dougherty, E., & Rasmussen, K. L. (2019). Climatology of flood-producing storms and their associated rainfall characteristics in the united states. *Monthly Weather Review*, *147*(11), 3861–3877.

Douville, H., Raghavan, J., R.P., R., Allan, P., Arias, M., Barlow, R., Cerezo-Mota, A., Cherchi, T., Gan, J., Gergis, D., Jiang, A., Khan, W., Pokam Mba, D., Rosenfeld, J., Tierney, & Zolina, O. (2021). Water cycle changes. in climate change 2021: The physical science basis. contribution of working group i to the sixth assessment report of the intergovernmental panel on climate change.

Ehlers, T. A., Chen, D., Appel, E., Bolch, T., Chen, F., Diekmann, B., Dippold, M. A., Giese, M., Guggenberger, G., Lai, H.-W., et al. (2022). Past, present, and future geo-biosphere interactions on the tibetan plateau and implications for permafrost. *Earth-Science Reviews*, 104197.

Fan, X., Wang, L., Li, X., Zhou, J., Chen, D., & Yang, H. (2022). Increased discharge across the yellow river basin in the 21st century was dominated by precipitation in the headwater region. *Journal of Hydrology: Regional Studies*, *44*, 101230.

Farr, T. G., Rosen, P. A., Caro, E., Crippen, R., Duren, R., Hensley, S., Kobrick, M., Paller, M., Rodriguez, E., Roth, L., et al. (2007). The shuttle radar topography mission. *Reviews of geophysics*, *45*(2).

Feng, Z., Leung, L. R., Liu, N., Wang, J., Houze Jr, R. A., Li, J., Hardin, J. C., Chen, D., & Guo, J. (2021). A global high-resolution mesoscale convective system database using satellite-derived cloud tops, surface precipitation, and tracking. *Journal of Geophysical Research: Atmospheres*, e2020JD034202.

Flohn, H. (1957). Large-scale aspects of the "summer monsoon" in south and east asia. *Journal of the Meteorological Society of Japan. Ser. II*, *35*, 180–186.

Flohn, H., & Reiter, E. R. (1968). *Contributions to a meteorology of the tibetan highlands* (Doctoral dissertation). Colorado State University. Libraries.

Funk, C., Peterson, P., Landsfeld, M., Pedreros, D., Verdin, J., Shukla, S., Husak, G., Rowland, J., Harrison, L., Hoell, A., et al. (2015). The climate hazards infrared precipitation with stations—a new environmental record for monitoring extremes. *Scientific data*, *2*(1), 1–21.

Gao, Y., Xiao, L., Chen, D., Xu, J., & Zhang, H. (2018). Comparison between past and future extreme precipitations simulated by global and regional climate models over the tibetan plateau. *International Journal of Climatology*, *38*(3), 1285–1297.

Giorgi, F., & Gutowski Jr, W. J. (2015). Regional dynamical downscaling and the cordex initiative. *Annual review of environment and resources*, *40*, 467–490.

Groisman, P. Y., & Easterling, D. R. (1994). Variability and trends of total precipitation and snowfall over the united states and canada. *Journal of Climate*, *7*(1), 184–205.

Harris, C. R., Millman, K. J., van der Walt, S. J., Gommers, R., Virtanen, P., Cournapeau, D., Wieser, E., Taylor, J., Berg, S., Smith, N. J., Kern, R., Picus, M., Hoyer, S., van Kerkwijk, M. H., Brett, M., Haldane, A., del Río, J. F., Wiebe, M., Peterson, P., . . . Oliphant, T. E. (2020). Array programming with NumPy. *Nature*, *585*(7825), 357–362. https://doi.org/10.1038/s41586-020-2649-2

Heikenfeld, M., Marinescu, P. J., Christensen, M., Watson-Parris, D., Senf, F., van den Heever, S. C., & Stier, P. (2019). Tobac 1.2: Towards a flexible framework for tracking and analysis of clouds in diverse datasets. *Geoscientific Model Development*, *12*(11), 4551–4570.

Hersbach, H., Bell, B., Berrisford, P., Hirahara, S., Horányi, A., Muñoz-Sabater, J., Nicolas, J., Peubey, C., Radu, R., Schepers, D., et al. (2020). The era5 global reanalysis. *Quarterly Journal of the Royal Meteorological Society*, *146*(730), 1999–2049.

Hitchcock, S. M., Schumacher, R. S., Herman, G. R., Coniglio, M. C., Parker, M. D., & Ziegler, C. L. (2019). Evolution of pre-and postconvective environmental profiles from mesoscale convective systems during pecan. *Monthly Weather Review*, *147*(7), 2329–2354.

Hock, R., Rasul, G., Adler, C., Cáceres, B., Gruber, S., Hirabayashi, Y., Jackson, M., Kääb, A., Kang, S., Kutuzov, S., et al. (2019). High mountain areas: In: Ipcc special report on the ocean and cryosphere in a changing climate.

Houze Jr, R. A. (1997). Stratiform precipitation in regions of convection: A meteorological paradox? *Bulletin of the American Meteorological Society*, *78*(10), 2179–2196.

Houze Jr, R. A. (2004). Mesoscale convective systems. *Reviews of Geophysics*, *42*(4).

Hoyer, S., & Hamman, J. (2017). Xarray: Nd labeled arrays and datasets in python. *Journal of Open Research Software*, *5*(1).

Hu, H., Feng, Z., & Leung, L.-Y. R. (2021). Linking flood frequency with mesoscale convective systems in the us. *Geophysical Research Letters*, *48*(9), e2021GL092546.

Hu, H., Leung, R., & Feng, Z. (2020). Observed warm-season characteristics of mcs and non-mcs rainfall and their recent changes in the central united states. *Geophysical Research Letters*, *47*(6), e2019GL086783.

Huffman, G., Stocker, E., Bolvin, D., Nelkin, E., & Jackson, T. (2019). Gpm imerg final precipitation l3 half hourly 0.1 degree x 0.1 degree v06. *Greenbelt, MD, Goddard Earth Sciences Data and Information Services Center (GES DISC).*

Hunter, J. D. (2007). Matplotlib: A 2d graphics environment. *Computing in Science & Engineering*, *9*(3), 90–95. https://doi.org/10.1109/MCSE.2007.55

Immerzeel, W. W., Lutz, A., Andrade, M., Bahl, A., Biemans, H., Bolch, T., Hyde, S., Brumby, S., Davies, B., Elmore, A., et al. (2020). Importance and vulnerability of the world's water towers. *Nature*, *577*(7790), 364–369.

Janowiak, J., Joyce, B., & Xie, P. (2017). Ncep/cpc l3 half hourly 4km global (60s - 60n) merged ir v1. *Edited by Andrey Savtchenko, Greenbelt, MD, Goddard Earth Sciences Data and Information Services Center (GES DISC).*

Joyce, R. J., Janowiak, J. E., Arkin, P. A., & Xie, P. (2004). Cmorph: A method that produces global precipitation estimates from passive microwave and infrared data at high spatial and temporal resolution. *Journal of hydrometeorology*, *5*(3), 487–503.

Kendon, E. J., Ban, N., Roberts, N. M., Fowler, H. J., Roberts, M. J., Chan, S. C., Evans, J. P., Fosser, G., & Wilkinson, J. M. (2017). Do convection-permitting regional climate models improve projections of future precipitation change? *Bulletin of the American Meteorological Society*, *98*(1), 79–93.

Kidd, C., & Huffman, G. (2011). Global precipitation measurement. *Meteorological Applications*, *18*(3), 334–353.

Lehner, B., & Grill, G. (2013). Global river hydrography and network routing: Baseline data and new approaches to study the world's large river systems. *Hydrological Processes*, *27*(15), 2171–2186.

Lenderink, G., Barbero, R., Loriaux, J., & Fowler, H. (2017). Super-clausius–clapeyron scaling of extreme hourly convective precipitation and its relation to large-scale atmospheric conditions. *Journal of Climate*, *30*(15), 6037–6052.

Li, P., Furtado, K., Zhou, T., Chen, H., & Li, J. (2021). Convection-permitting modelling improves simulated precipitation over the central and eastern tibetan plateau. *Quarterly Journal of the Royal Meteorological Society*, *147*(734), 341–362.

Lin, C., Chen, D., Yang, K., & Ou, T. (2018). Impact of model resolution on simulating the water vapor transport through the central himalayas: Implication for models' wet bias over the tibetan plateau. *Climate dynamics*, *51*, 3195–3207.

Lohmann, U., Lüönd, F., & Mahrt, F. (2016). *An introduction to clouds: From the microscale to climate*. Cambridge University Press.

Lucas-Picher, P., Argüeso, D., Brisson, E., Tramblay, Y., Berg, P., Lemonsu, A., Kotlarski, S., & Caillaud, C. (2021). Convection-permitting modeling with regional climate models: Latest developments and next steps. *Wiley Interdisciplinary Reviews: Climate Change*, *12*(6), e731.

Met Office. (2010 - 2013). *Cartopy: A cartographic python library with matplotlib support*. Exeter, Devon. https://scitools.org.uk/cartopy

Musselman, K. N., Lehner, F., Ikeda, K., Clark, M. P., Prein, A. F., Liu, C., Barlage, M., & Rasmussen, R. (2018). Projected increases and shifts in rain-on-snow flood risk over western north america. *Nature Climate Change*, *8*(9), 808–812.

O'Gorman, P. A. (2015). Precipitation extremes under climate change. *Current climate change reports*, *1*(2), 49–59.

O'Gorman, P. A., Allan, R. P., Byrne, M. P., & Previdi, M. (2012). Energetic constraints on precipitation under climate change. *Surveys in geophysics*, *33*(3), 585–608.

Orlanski, I. (1975). A rational subdivision of scales for atmospheric processes. *Bulletin of the American Meteorological Society*, 527–530.

Orr, H., Ekström, M., Charlton, M., Peat, K., & Fowler, H. (2021). Using high-resolution climate change information in water management: A decision-makers' perspective. *Philosophical Transactions of the Royal Society A*, *379*(2195), 20200219.

Ou, T., Chen, D., Chen, X., Lin, C., Yang, K., Lai, H.-W., & Zhang, F. (2020). Simulation of summer precipitation diurnal cycles over the tibetan plateau at the gray-zone grid spacing for cumulus parameterization. *Climate Dynamics*, *54*(7), 3525–3539.

Ou, T., Chen, D., Tang, J., Lin, C., Wang, X., Kukulies, J., & Lai, H.-W. (2023). Wet bias of summer precipitation in the northwestern tibetan plateau in era5 is linked to overestimated lower-level southerly wind over the plateau. *Climate Dynamics*, 1–15.

pandas development team, T. (2020). *Pandas-dev/pandas: Pandas* (Version latest). Zenodo. https://doi.org/10.5281/zenodo.3509134

Peixoto, J. P., & Oort, A. H. (1992). Physics of climate.

Pendergrass, A. G. (2020). Changing degree of convective organization as a mechanism for dynamic changes in extreme precipitation. *Current climate change reports*, *6*(2), 47–54.

Pepin, N., Bradley, R. S., Diaz, H., Baraër, M., Caceres, E., Forsythe, N., Fowler, H., Greenwood, G., Hashmi, M., Liu, X., et al. (2015). Elevation-dependent warming in mountain regions of the world. *Nature climate change*, *5*(5), 424–430.

Pörtner, H.-O., Roberts, D. C., Adams, H., Adler, C., Aldunce, P., Ali, E., Begum, R. A., Betts, R., Kerr, R. B., Biesbroek, R., et al. (2022). *Climate change 2022: Impacts, adaptation and vulnerability*. IPCC Geneva, Switzerland:

Prein, A., Rasmussen, R., Wang, D., & Giangrande, S. (2021). Sensitivity of organized convective storms to model grid spacing in current and future climates. *Philosophical Transactions of the Royal Society A*, *379*(2195), 20190546.

Prein, A. F., Ban, N., Ou, T., Tang, J., Sakaguchi, K., Collier, E., Jayanarayanan, S., Li, L., Sobolowski, S., Chen, X., et al. (2022). Towards ensemble-based kilometer-scale climate simulations over the third pole region.

Prein, A. F., Langhans, W., Fosser, G., Ferrone, A., Ban, N., Goergen, K., Keller, M., Tölle, M., Gutjahr, O., Feser, F., et al. (2015). A review on regional convection-permitting climate modeling: Demonstrations, prospects, and challenges. *Reviews of geophysics*, *53*(2), 323–361.

Prein, A. F., Liu, C., Ikeda, K., Bullock, R., Rasmussen, R. M., Holland, G. J., & Clark, M. (2020). Simulating north american mesoscale convective systems with a convection-permitting climate model. *Climate Dynamics*, *55*(1), 95–110.

Prein, A. F., Liu, C., Ikeda, K., Trier, S. B., Rasmussen, R. M., Holland, G. J., & Clark, M. P. (2017). Increased rainfall volume from future convective storms in the us. *Nature Climate Change*, *7*(12), 880–884.

Prein, A. F., Rasmussen, R., & Stephens, G. (2017). Challenges and advances in convection-permitting climate modeling. *Bulletin of the American Meteorological Society*, *98*(5), 1027–1030.

Prein, A. F., Rasmussen, R. M., Ikeda, K., Liu, C., Clark, M. P., & Holland, G. J. (2017). The future intensification of hourly precipitation extremes. *Nature Climate Change*, *7*(1), 48–52.

Rasmussen, K., & Houze Jr, R. (2016). Convective initiation near the andes in subtropical south america. *Monthly Weather Review*, *144*(6), 2351–2374.

Rasmussen, K. L., & Houze, R. A. (2011). Orogenic convection in subtropical south america as seen by the trmm satellite. *Monthly Weather Review*, *139*(8), 2399–2420.

Rasmussen, K. L., Prein, A. F., Rasmussen, R. M., Ikeda, K., & Liu, C. (2020). Changes in the convective population and thermodynamic environments in convection-permitting regional climate simulations over the united states. *Climate Dynamics*, *55*, 383–408.

Rasmussen, R., Baker, B., Kochendorfer, J., Meyers, T., Landolt, S., Fischer, A. P., Black, J., Thériault, J. M., Kucera, P., Gochis, D., et al. (2012). How well are we measuring snow: The noaa/faa/ncar winter precipitation test bed. *Bulletin of the American Meteorological Society*, *93*(6), 811–829.

Schiemann, R., Lüthi, D., & Schär, C. (2009). Seasonality and interannual variability of the westerly jet in the tibetan plateau region. *Journal of climate*, *22*(11), 2940–2957.

Schumacher, R. S., & Rasmussen, K. L. (2020). The formation, character and changing nature of mesoscale convective systems. *Nature Reviews Earth & Environment*, *1*(6), 300–314.

Shukla, J., Brunet, G., Nobre, C., Béland, M., Dole, R., Trenberth, K., Anthes, R., Asrar, G., Barrie, L., Bougeault, P., et al. (2021). An earth-system prediction initiative for the 21 st century.

Skamarock, W. C., Klemp, J. B., Dudhia, J., Gill, D. O., Liu, Z., Berner, J., Wang, W., Powers, J. G., Duda, M. G., Barker, D. M., et al. (2019). A description of the advanced research wrf model version 4. *National Center for Atmospheric Research: Boulder, CO, USA*, *145*(145), 550.

Smith, A. B., et al. (2020). Us billion-dollar weather and climate disasters, 1980–present (ncei accession 0209268). *NOAA National Centers for Environmental Information*, *10*.

Song, F., Feng, Z., Leung, L. R., Pokharel, B., Wang, S.-Y. S., Chen, X., Sakaguchi, K., & Wang, C.-c. (2021). Crucial roles of eastward propagating environments in the summer mcs initiation over the us great plains. *Journal of Geophysical Research: Atmospheres*, *126*(16), e2021JD034991.

Stephens, G. L., Vane, D. G., Boain, R. J., Mace, G. G., Sassen, K., Wang, Z., Illingworth, A. J., O'connor, E. J., Rossow, W. B., Durden, S. L., et al. (2002). The cloudsat mission and the a-train: A new dimension of space-based observations of clouds and precipitation. *Bulletin of the American Meteorological Society*, *83*(12), 1771–1790.

Sugimoto, S., & Ueno, K. (2012). Role of mesoscale convective systems developed around the eastern tibetan plateau in the eastward expansion of an upper tropospheric high during the monsoon season. *Journal of the Meteorological Society of Japan. Ser. II*, *90*(2), 297–310.

Trapp, R. J. (2013). *Mesoscale-convective processes in the atmosphere*. Cambridge University Press.

Virtanen, P., Gommers, R., Oliphant, T. E., Haberland, M., Reddy, T., Cournapeau, D., Burovski, E., Peterson, P., Weckesser, W., Bright, J., van der Walt, S. J., Brett, M., Wilson, J., Millman, K. J., Mayorov, N., Nelson, A. R. J., Jones, E., Kern, R., Larson, E., ... SciPy 1.0 Contributors. (2020). SciPy 1.0: Fundamental Algorithms for Scientific Computing in Python. *Nature Methods*, *17*, 261–272. https://doi.org/10.1038/s41592-019-0686-2

Wang, S.-Y., Chen, T.-C., & Takle, E. S. (2011). Climatology of summer midtropospheric perturbations in the us northern plains. part ii: Large-scale effects of the rocky mountains on genesis. *Climate dynamics*, *36*(7), 1221–1237.

Westerling, A. L. (2016). Increasing western us forest wildfire activity: Sensitivity to changes in the timing of spring. *Philosophical Transactions of the Royal Society B: Biological Sciences*, *371*(1696), 20150178.

Yao, T., Bolch, T., Chen, D., Gao, J., Immerzeel, W., Piao, S., Su, F., Thompson, L., Wada, Y., Wang, L., et al. (2022). The imbalance of the asian water tower. *Nature Reviews Earth & Environment*, 1–15.

Yao, T., Masson-Delmotte, V., Gao, J., Yu, W., Yang, X., Risi, C., Sturm, C., Werner, M., Zhao, H., He, Y., et al. (2013). A review of climatic controls on δ18o in precipitation over the tibetan plateau: Observations and simulations. *Reviews of Geophysics*, *51*(4), 525–548.

Ye, D.-Z., & Wu, G.-X. (1998). The role of the heat source of the tibetan plateau in the general circulation. *Meteorology and Atmospheric Physics*, *67*(1), 181–198.

Yeh, T. (1982). Some aspects of the thermal influences of the qinghai-tibetan plateau on the atmospheric circulation. *Archives for meteorology, geophysics, and bioclimatology, Series A*, *31*(3), 205–220.

Zhou, X., Yang, K., Ouyang, L., Wang, Y., Jiang, Y., Li, X., Chen, D., & Prein, A. (2021). Added value of kilometer-scale modeling over the third pole region: A cordex-cptp pilot study. *Climate Dynamics*, 1–15.

Part II

APPENDED PAPERS